

Triplet structure of nuclear scissors mode

E.B. Balbutsev, I.V. Molodtsova, A.V. Sushkov, N.Yu. Shirikova
Joint Institute for Nuclear Research, 141980 Dubna, Moscow Region, Russia

P. Schuck
Institut de Physique Nucléaire, IN2P3-CNRS,
Université Paris-Sud, F-91406 Orsay Cédex, France;
Univ. Grenoble Alpes, CNRS, LPMMC, 38000 Grenoble, France

The fine structure of the scissors mode is investigated within the Time Dependent Hartree-Fock-Bogoliubov (TDHFB) approach. The solution of TDHFB equations by the Wigner Function Moments (WFM) method predicts a splitting of the scissors mode into three intermingled branches. Together with the conventional scissors mode two new modes arise due to spin degrees of freedom. They generate significant $M1$ strength below the conventional energy range. The results of calculations of scissors resonances in Rare Earths and Actinides by WFM and QPNM methods are compared with experimental data. A remarkable coherence of both methods together with experimental data is observed.

PACS numbers: 21.10.Hw, 21.60.Ev, 21.60.Jz, 24.30.Cz

Keywords: spin; pairing; collective motion; scissors mode; giant resonances

I. INTRODUCTION

In the review [1] it is stated that the scissors mode is "weakly collective, but strong on the single-particle scale" and further: "*The weakly collective scissors mode excitation has become an ideal test of models – especially microscopic models – of nuclear vibrations. Most models are usually calibrated to reproduce properties of strongly collective excitations (e.g. of $J^\pi = 2^+$ or 3^- states, giant resonances, ...). Weakly-collective phenomena, however, force the models to make genuine predictions and the fact that the transitions in question are strong on the single-particle scale makes it impossible to dismiss failures as a mere detail, especially in the light of the overwhelming experimental evidence for them in many nuclei [2, 3].*"

The Wigner Function Moments (WFM) or phase space moments method [4, 5] turns out to be very useful in this situation. On the one hand it is a purely microscopic method, because it is based on the Time Dependent Hartree-Fock (TDHF) equation. On the other hand the method works with average values (moments) of operators which have a direct relation to the considered phenomenon and, thus, make a natural bridge with the macroscopic description. This makes it an ideal instrument to describe the basic characteristics (energies and excitation probabilities) of collective excitations such as, in particular, the scissors mode.

In Ref. [6] the WFM method was applied for the first time to solve the TDHF equations including spin dynamics. The most remarkable result was the prediction of a new type of nuclear collective motion: rotational oscillations of "spin-up" nucleons with respect of "spin-down" nucleons (the spin scis-

sors mode).

A generalization of the WFM method which takes into account spin degrees of freedom and pair correlations simultaneously was outlined in [7], where the Time Dependent Hartree-Fock-Bogoliubov (TDHFB) equations were considered. As a result the agreement between theory and experiment in the description of nuclear scissors modes was improved considerably. The evolution of our results in comparison with experimental data is shown on Fig. 1.

By definition the scissors mode is a pure isovector mode. That is why we divided (approximately) the dynamical equations describing collective motion into isovector and isoscalar parts with the aim to separate the pure scissors mode.

To study the interplay of isovector and isoscalar low-lying 1^+ excitations we solved the coupled dynamical equations of our model for protons and neutrons exactly, without the artificial isovector-isoscalar decoupling. As a result one more magnetic mode (third type of scissors) appeared. Actually, the possible existence of three scissors states is easily explained by the combinatoric consideration – there are only three ways to divide the four different kinds of objects (spin up and spin down protons and neutrons in our case) into two pairs. The analysis of the new situation, which appeared due to the last findings in the description of nuclear scissors, is presented in this paper.

The paper is organized as follows. In Sec. II the TDHFB equations for the 2×2 normal and anomalous density matrices are formulated and their Wigner transform is found. In Sec. III the model Hamiltonian and the mean field are analyzed. In Sec. IV the collective variables are defined and the respective dynamical equations are derived. In

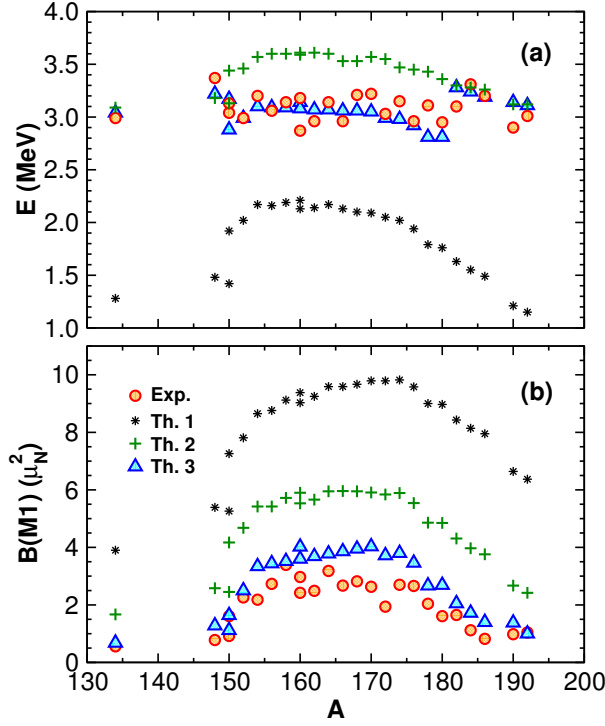


FIG. 1: Energy centroids E (a) and summed $B(M1)$ values (b) of the scissors mode. Th. 1 – the results of calculations without spin degrees of freedom and pair correlations, Th. 2 – pairing is included, Th. 3 – pairing and spin degrees of freedom are taken into account.

Sec. V the results of calculations of energies, $B(M1)$ values and currents for nuclei of the $N = 82 - 126$ mass region and Actinides are discussed. The summary of main results is given in the Conclusion section. The mathematical details can be found in Appendix.

II. WIGNER TRANSFORMATION OF TDHFB EQUATIONS

The TDHFB equations in matrix formulation [8, 9] are

$$i\hbar\dot{\mathcal{R}} = [\mathcal{H}, \mathcal{R}] \quad (1)$$

with

$$\mathcal{R} = \begin{pmatrix} \hat{\rho} & -\hat{\kappa} \\ -\hat{\kappa}^\dagger & 1 - \hat{\rho}^* \end{pmatrix}, \quad \mathcal{H} = \begin{pmatrix} \hat{h} & \hat{\Delta} \\ \hat{\Delta}^\dagger & -\hat{h}^* \end{pmatrix} \quad (2)$$

The normal density matrix $\hat{\rho}$ and Hamiltonian \hat{h} are hermitian whereas the abnormal density $\hat{\kappa}$ and the pairing gap $\hat{\Delta}$ are skew symmetric: $\hat{\kappa}^\dagger = -\hat{\kappa}^*$, $\hat{\Delta}^\dagger = -\hat{\Delta}^*$. The detailed form of the TDHFB equations is

$$\begin{aligned} i\hbar\dot{\hat{\rho}} &= \hat{h}\hat{\rho} - \hat{\rho}\hat{h} - \hat{\Delta}\hat{\kappa}^\dagger + \hat{\kappa}\hat{\Delta}^\dagger, \\ -i\hbar\dot{\hat{\rho}}^* &= \hat{h}^*\hat{\rho}^* - \hat{\rho}^*\hat{h}^* - \hat{\Delta}^\dagger\hat{\kappa} + \hat{\kappa}^\dagger\hat{\Delta}, \\ -i\hbar\dot{\hat{\kappa}} &= -\hat{h}\hat{\kappa} - \hat{\kappa}\hat{h}^* + \hat{\Delta} - \hat{\Delta}\hat{\rho}^* - \hat{\rho}\hat{\Delta}, \\ -i\hbar\dot{\hat{\kappa}}^\dagger &= \hat{h}^*\hat{\kappa}^\dagger + \hat{\kappa}^\dagger\hat{h} - \hat{\Delta}^\dagger + \hat{\Delta}^\dagger\hat{\rho} + \hat{\rho}^*\hat{\Delta}^\dagger. \end{aligned} \quad (3)$$

It is easy to see that the second and fourth equations are complex conjugate to the first and third ones respectively. Let us consider their matrix form in coordinate space keeping all spin indices s, s' : $\langle \mathbf{r}, s | \hat{\rho} | \mathbf{r}', s' \rangle$, $\langle \mathbf{r}, s | \hat{\kappa} | \mathbf{r}', s' \rangle$, etc. We do not specify the isospin indices in order to make formulae more transparent. They will be re-introduced later. Let us introduce the more compact notation $\langle \mathbf{r}, s | \hat{X} | \mathbf{r}', s' \rangle = X_{rr'}^{ss'}$. Then the set of TDHFB equations (3) with specified spin indices reads

$$\begin{aligned} i\hbar\dot{\rho}_{rr'}^{\uparrow\uparrow} &= \int d^3r' (h_{rr'}^{\uparrow\uparrow}\rho_{r'r''}^{\uparrow\uparrow} - \rho_{rr'}^{\uparrow\uparrow}h_{r'r''}^{\uparrow\uparrow} + \hat{h}_{rr'}^{\uparrow\downarrow}\rho_{r'r''}^{\uparrow\downarrow} - \rho_{rr'}^{\uparrow\downarrow}h_{r'r''}^{\uparrow\downarrow} - \Delta_{rr'}^{\uparrow\downarrow}\kappa_{r'r''}^{\uparrow\downarrow} + \kappa_{rr'}^{\uparrow\downarrow}\Delta_{r'r''}^{\uparrow\downarrow}), \\ i\hbar\dot{\rho}_{rr'}^{\uparrow\downarrow} &= \int d^3r' (h_{rr'}^{\uparrow\uparrow}\rho_{r'r''}^{\uparrow\downarrow} - \rho_{rr'}^{\uparrow\uparrow}h_{r'r''}^{\uparrow\downarrow} + \hat{h}_{rr'}^{\uparrow\downarrow}\rho_{r'r''}^{\downarrow\downarrow} - \rho_{rr'}^{\uparrow\downarrow}h_{r'r''}^{\downarrow\downarrow}), \\ i\hbar\dot{\rho}_{rr'}^{\downarrow\uparrow} &= \int d^3r' (h_{rr'}^{\downarrow\downarrow}\rho_{r'r''}^{\downarrow\uparrow} - \rho_{rr'}^{\downarrow\downarrow}h_{r'r''}^{\downarrow\uparrow} + \hat{h}_{rr'}^{\downarrow\uparrow}\rho_{r'r''}^{\downarrow\uparrow} - \rho_{rr'}^{\downarrow\uparrow}h_{r'r''}^{\downarrow\uparrow}), \\ i\hbar\dot{\rho}_{rr'}^{\downarrow\downarrow} &= \int d^3r' (h_{rr'}^{\downarrow\downarrow}\rho_{r'r''}^{\downarrow\downarrow} - \rho_{rr'}^{\downarrow\downarrow}h_{r'r''}^{\downarrow\downarrow} + \hat{h}_{rr'}^{\downarrow\uparrow}\rho_{r'r''}^{\downarrow\uparrow} - \rho_{rr'}^{\downarrow\uparrow}h_{r'r''}^{\downarrow\uparrow} - \Delta_{rr'}^{\downarrow\uparrow}\kappa_{r'r''}^{\downarrow\uparrow} + \kappa_{rr'}^{\downarrow\uparrow}\Delta_{r'r''}^{\downarrow\uparrow}), \\ i\hbar\dot{\kappa}_{rr'}^{\uparrow\downarrow} &= -\hat{\Delta}_{rr'}^{\uparrow\downarrow} + \int d^3r' (h_{rr'}^{\uparrow\uparrow}\kappa_{r'r''}^{\uparrow\downarrow} + \kappa_{rr'}^{\uparrow\downarrow}h_{r'r''}^{\downarrow\downarrow} + \Delta_{rr'}^{\uparrow\downarrow}\rho_{r'r''}^{\downarrow\downarrow} + \rho_{rr'}^{\uparrow\uparrow}\Delta_{r'r''}^{\uparrow\downarrow}), \\ i\hbar\dot{\kappa}_{rr'}^{\downarrow\uparrow} &= -\hat{\Delta}_{rr'}^{\downarrow\uparrow} + \int d^3r' (h_{rr'}^{\downarrow\downarrow}\kappa_{r'r''}^{\downarrow\uparrow} + \kappa_{rr'}^{\downarrow\uparrow}h_{r'r''}^{\downarrow\uparrow} + \Delta_{rr'}^{\downarrow\uparrow}\rho_{r'r''}^{\downarrow\uparrow} + \rho_{rr'}^{\downarrow\downarrow}\Delta_{r'r''}^{\downarrow\uparrow}). \end{aligned} \quad (4)$$

This set of equations must be complemented by the complex conjugated equations. Writing these equations we neglected the diagonal in spin matrix elements of the abnormal density: $\kappa_{rr'}^{ss}$ and $\Delta_{rr'}^{ss}$. It was shown in [7] that such an approximation works very well in the case of monopole pairing considered here.

We will work with the Wigner transform [9] of equations (4). From now on, we will not write out the coordinate dependence (\mathbf{r}, \mathbf{p}) of all functions in order to make the formulae more transparent. We have

$$\begin{aligned}
i\hbar f^{\uparrow\uparrow} &= i\hbar\{h^{\uparrow\uparrow}, f^{\uparrow\uparrow}\} + h^{\uparrow\downarrow}f^{\downarrow\uparrow} - f^{\uparrow\downarrow}h^{\downarrow\uparrow} + \frac{i\hbar}{2}\{h^{\uparrow\downarrow}, f^{\downarrow\uparrow}\} - \frac{i\hbar}{2}\{f^{\uparrow\downarrow}, h^{\downarrow\uparrow}\} \\
&- \frac{\hbar^2}{8}\{\{h^{\uparrow\downarrow}, f^{\downarrow\uparrow}\}\} + \frac{\hbar^2}{8}\{\{f^{\uparrow\downarrow}, h^{\downarrow\uparrow}\}\} + \kappa\Delta^* - \Delta\kappa^* \\
&+ \frac{i\hbar}{2}\{\kappa, \Delta^*\} - \frac{i\hbar}{2}\{\Delta, \kappa^*\} - \frac{\hbar^2}{8}\{\{\kappa, \Delta^*\}\} + \frac{\hbar^2}{8}\{\{\Delta, \kappa^*\}\} + \dots, \\
i\hbar f^{\downarrow\downarrow} &= i\hbar\{h^{\downarrow\downarrow}, f^{\downarrow\downarrow}\} + h^{\downarrow\uparrow}f^{\uparrow\downarrow} - f^{\downarrow\uparrow}h^{\uparrow\downarrow} + \frac{i\hbar}{2}\{h^{\downarrow\uparrow}, f^{\uparrow\downarrow}\} - \frac{i\hbar}{2}\{f^{\downarrow\uparrow}, h^{\uparrow\downarrow}\} \\
&- \frac{\hbar^2}{8}\{\{h^{\downarrow\uparrow}, f^{\uparrow\downarrow}\}\} + \frac{\hbar^2}{8}\{\{f^{\downarrow\uparrow}, h^{\uparrow\downarrow}\}\} + \bar{\Delta}^*\bar{\kappa} - \bar{\kappa}^*\bar{\Delta} \\
&+ \frac{i\hbar}{2}\{\bar{\Delta}^*, \bar{\kappa}\} - \frac{i\hbar}{2}\{\bar{\kappa}^*, \bar{\Delta}\} - \frac{\hbar^2}{8}\{\{\bar{\Delta}^*, \bar{\kappa}\}\} + \frac{\hbar^2}{8}\{\{\bar{\kappa}^*, \bar{\Delta}\}\} + \dots, \\
i\hbar f^{\uparrow\downarrow} &= f^{\uparrow\downarrow}(h^{\uparrow\uparrow} - h^{\downarrow\downarrow}) + \frac{i\hbar}{2}\{(h^{\uparrow\uparrow} + h^{\downarrow\downarrow}), f^{\uparrow\downarrow}\} - \frac{\hbar^2}{8}\{\{(h^{\uparrow\uparrow} - h^{\downarrow\downarrow}), f^{\uparrow\downarrow}\}\} \\
&- h^{\uparrow\downarrow}(f^{\uparrow\uparrow} - f^{\downarrow\downarrow}) + \frac{i\hbar}{2}\{h^{\uparrow\downarrow}, (f^{\uparrow\uparrow} + f^{\downarrow\downarrow})\} + \frac{\hbar^2}{8}\{\{h^{\uparrow\downarrow}, (f^{\uparrow\uparrow} - f^{\downarrow\downarrow})\}\} + \dots, \\
i\hbar f^{\downarrow\uparrow} &= f^{\downarrow\uparrow}(h^{\downarrow\downarrow} - h^{\uparrow\uparrow}) + \frac{i\hbar}{2}\{(h^{\downarrow\downarrow} + h^{\uparrow\uparrow}), f^{\downarrow\uparrow}\} - \frac{\hbar^2}{8}\{\{(h^{\downarrow\downarrow} - h^{\uparrow\uparrow}), f^{\downarrow\uparrow}\}\} \\
&- h^{\downarrow\uparrow}(f^{\downarrow\downarrow} - f^{\uparrow\uparrow}) + \frac{i\hbar}{2}\{h^{\downarrow\uparrow}, (f^{\downarrow\downarrow} + f^{\uparrow\uparrow})\} + \frac{\hbar^2}{8}\{\{h^{\downarrow\uparrow}, (f^{\downarrow\downarrow} - f^{\uparrow\uparrow})\}\} + \dots, \\
i\hbar\kappa &= \kappa(h^{\uparrow\uparrow} + \bar{h}^{\downarrow\downarrow}) + \frac{i\hbar}{2}\{(h^{\uparrow\uparrow} - \bar{h}^{\downarrow\downarrow}), \kappa\} - \frac{\hbar^2}{8}\{\{(h^{\uparrow\uparrow} + \bar{h}^{\downarrow\downarrow}), \kappa\}\} \\
&+ \Delta(f^{\uparrow\uparrow} + \bar{f}^{\downarrow\downarrow}) + \frac{i\hbar}{2}\{(f^{\uparrow\uparrow} - \bar{f}^{\downarrow\downarrow}), \Delta\} - \frac{\hbar^2}{8}\{\{(f^{\uparrow\uparrow} + \bar{f}^{\downarrow\downarrow}), \Delta\}\} - \Delta + \dots, \\
i\hbar\kappa^* &= -\kappa^*(h^{\uparrow\uparrow} + \bar{h}^{\downarrow\downarrow}) + \frac{i\hbar}{2}\{(h^{\uparrow\uparrow} - \bar{h}^{\downarrow\downarrow}), \kappa^*\} + \frac{\hbar^2}{8}\{\{(h^{\uparrow\uparrow} + \bar{h}^{\downarrow\downarrow}), \kappa^*\}\} \\
&- \Delta^*(f^{\uparrow\uparrow} + \bar{f}^{\downarrow\downarrow}) + \frac{i\hbar}{2}\{(f^{\uparrow\uparrow} - \bar{f}^{\downarrow\downarrow}), \Delta^*\} + \frac{\hbar^2}{8}\{\{(f^{\uparrow\uparrow} + \bar{f}^{\downarrow\downarrow}), \Delta^*\}\} + \Delta^* + \dots, \tag{5}
\end{aligned}$$

where the functions h , f , Δ , and κ are the Wigner transforms of \hat{h} , $\hat{\rho}$, $\hat{\Delta}$, and $\hat{\kappa}$, respectively, $\bar{f}(\mathbf{r}, \mathbf{p}) = f(\mathbf{r}, -\mathbf{p})$, $\{f, g\}$ is the Poisson bracket of the functions f and g and $\{\{f, g\}\}$ is their double Poisson bracket, $f(\mathbf{r}, \mathbf{p})$ being the Wigner function. This set of equations must be complemented by the dynamical equations for $\bar{f}^{\uparrow\uparrow}$, $\bar{f}^{\downarrow\downarrow}$, $\bar{f}^{\uparrow\downarrow}$, $\bar{f}^{\downarrow\uparrow}$, $\bar{\kappa}$, $\bar{\kappa}^*$. They are obtained by the change $\mathbf{p} \rightarrow -\mathbf{p}$ in arguments of functions and Poisson brackets. We introduced the notation $\kappa \equiv \kappa^{\uparrow\downarrow}$ and $\Delta \equiv \Delta^{\uparrow\downarrow}$. Symmetry properties of matrices $\hat{\kappa}$, $\hat{\Delta}$ and the properties of their Wigner transforms (see [7]) allow us to replace the functions $\kappa^{\downarrow\uparrow}(\mathbf{r}, \mathbf{p})$ and $\Delta^{\downarrow\uparrow}(\mathbf{r}, \mathbf{p})$ by the functions $\bar{\kappa}^{\uparrow\downarrow}(\mathbf{r}, \mathbf{p})$ and $\bar{\Delta}^{\uparrow\downarrow}(\mathbf{r}, \mathbf{p})$. The dots stand for terms proportional to higher powers of \hbar – after integration over phase space these terms disappear and we arrive to the set of exact integral equations. Following the paper [6] above equations can be rewritten in terms of spin-scalar $f^+ = f^{\uparrow\uparrow} + f^{\downarrow\downarrow}$ and spin-vector $f^- = f^{\uparrow\downarrow} - f^{\downarrow\uparrow}$ functions. Furthermore, it is useful to rewrite the obtained equations in terms of even and odd functions $f_e = \frac{1}{2}(f + \bar{f})$ and $f_o = \frac{1}{2}(f - \bar{f})$ and real and imaginary parts of κ and Δ : $\kappa^r = \frac{1}{2}(\kappa + \kappa^*)$, $\kappa^i = \frac{1}{2i}(\kappa - \kappa^*)$, $\Delta^r = \frac{1}{2}(\Delta + \Delta^*)$, $\Delta^i = \frac{1}{2i}(\Delta - \Delta^*)$. These operations are straightforward and omitted here.

III. MODEL HAMILTONIAN

The microscopic Hamiltonian of the model, harmonic oscillator with spin orbit potential plus separable quadrupole-quadrupole and spin-spin residual interactions is given by

$$H = \sum_{i=1}^A \left[\frac{\hat{\mathbf{p}}_i^2}{2m} + \frac{1}{2}m\omega^2\mathbf{r}_i^2 - \eta\hat{\mathbf{l}}_i\hat{\mathbf{S}}_i \right] + H_{qq} + H_{ss} \tag{6}$$

with

$$H_{qq} = \sum_{\mu=-2}^2 (-1)^\mu \left\{ \bar{\kappa} \sum_i^Z \sum_j^N + \frac{\kappa}{2} \left[\sum_{i,j(i \neq j)}^Z + \sum_{i,j(i \neq j)}^N \right] \right\} q_{2-\mu}(\mathbf{r}_i) q_{2\mu}(\mathbf{r}_j), \quad (7)$$

$$H_{ss} = \sum_{\mu=-1}^1 (-1)^\mu \left\{ \bar{\chi} \sum_i^Z \sum_j^N + \frac{\chi}{2} \left[\sum_{i,j(i \neq j)}^Z + \sum_{i,j(i \neq j)}^N \right] \right\} \hat{S}_{-\mu}(i) \hat{S}_\mu(j) \delta(\mathbf{r}_i - \mathbf{r}_j), \quad (8)$$

where $q_{2\mu} = \sqrt{16\pi/5} r^2 Y_{2\mu} = \sqrt{6} \{r \otimes r\}_{\lambda\mu}$, $\{r \otimes r\}_{\lambda\mu} = \sum_{\sigma,\nu} C_{1\sigma,1\nu}^{\lambda\mu} r_\sigma r_\nu$, $C_{1\sigma,1\nu}^{\lambda\mu}$ is the Clebsch-Gordan coefficient, cyclic coordinates r_{-1}, r_0, r_1 are defined in [10], N and Z are the numbers of neutrons and protons. \hat{S}_μ are spin matrices [10]:

$$\hat{S}_1 = -\frac{\hbar}{\sqrt{2}} \begin{pmatrix} 0 & 1 \\ 0 & 0 \end{pmatrix}, \quad \hat{S}_0 = \frac{\hbar}{2} \begin{pmatrix} 1 & 0 \\ 0 & -1 \end{pmatrix}, \quad \hat{S}_{-1} = \frac{\hbar}{\sqrt{2}} \begin{pmatrix} 0 & 0 \\ 1 & 0 \end{pmatrix}. \quad (9)$$

A. Mean Field

Let us analyze the mean field generated by this Hamiltonian.

1. Spin-orbit Potential

Written in cyclic coordinates, the spin orbit part of the Hamiltonian reads

$$\hat{h}_{ls} = -\eta \sum_{\mu=-1}^1 (-)^\mu \hat{l}_\mu \hat{S}_{-\mu} = -\eta \begin{pmatrix} \hat{l}_0 \frac{\hbar}{2} & \hat{l}_{-1} \frac{\hbar}{\sqrt{2}} \\ -\hat{l}_1 \frac{\hbar}{\sqrt{2}} & -\hat{l}_0 \frac{\hbar}{2} \end{pmatrix},$$

where [10]

$$\hat{l}_\mu = -\hbar \sqrt{2} \sum_{\nu,\alpha} C_{1\nu,1\alpha}^{1\mu} r_\nu \nabla_\alpha, \quad (10)$$

and

$$\begin{aligned} \hat{l}_1 &= \hbar(r_0 \nabla_1 - r_1 \nabla_0) = -\frac{1}{\sqrt{2}}(\hat{l}_x + i\hat{l}_y), \\ \hat{l}_0 &= \hbar(r_{-1} \nabla_1 - r_1 \nabla_{-1}) = \hat{l}_z, \\ \hat{l}_{-1} &= \hbar(r_{-1} \nabla_0 - r_0 \nabla_{-1}) = \frac{1}{\sqrt{2}}(\hat{l}_x - i\hat{l}_y), \\ \hat{l}_x &= -i\hbar(y \nabla_z - z \nabla_y), \quad \hat{l}_y = -i\hbar(z \nabla_x - x \nabla_z), \\ \hat{l}_z &= -i\hbar(x \nabla_y - y \nabla_x), \end{aligned} \quad (11)$$

$\eta = 2\hbar \dot{\omega}_0 \kappa_{\text{Nils}}$. The matrix elements of \hat{h}_{ls} in coordinate space can be written [6] as

$$\begin{aligned} \langle \mathbf{r}_1, s_1 | \hat{h}_{ls} | \mathbf{r}_2, s_2 \rangle &= -\frac{\hbar}{2} \eta \left[\hat{l}_0(\mathbf{r}_1) (\delta_{s_1 \uparrow} \delta_{s_2 \uparrow} - \delta_{s_1 \downarrow} \delta_{s_2 \downarrow}) \right. \\ &+ \left. \sqrt{2} \hat{l}_{-1}(\mathbf{r}_1) \delta_{s_1 \uparrow} \delta_{s_2 \downarrow} - \sqrt{2} \hat{l}_1(\mathbf{r}_1) \delta_{s_1 \downarrow} \delta_{s_2 \uparrow} \right] \delta(\mathbf{r}_1 - \mathbf{r}_2). \end{aligned}$$

Their Wigner transform reads [6]:

$$\begin{aligned} h_{ls}^{s_1 s_2}(\mathbf{r}, \mathbf{p}) &= -\frac{\hbar}{2} \eta \left[l_0(\mathbf{r}, \mathbf{p}) (\delta_{s_1 \uparrow} \delta_{s_2 \uparrow} - \delta_{s_1 \downarrow} \delta_{s_2 \downarrow}) \right. \\ &+ \left. \sqrt{2} l_{-1}(\mathbf{r}, \mathbf{p}) \delta_{s_1 \uparrow} \delta_{s_2 \downarrow} - \sqrt{2} l_1(\mathbf{r}, \mathbf{p}) \delta_{s_1 \downarrow} \delta_{s_2 \uparrow} \right], \end{aligned} \quad (12)$$

with $l_\mu(\mathbf{r}, \mathbf{p}) = -i\sqrt{2} \sum_{\nu,\alpha} C_{1\nu,1\alpha}^{1\mu} r_\nu p_\alpha$.

2. Quadrupole-quadrupole interaction

The contribution of H_{qq} to the mean field potential is easily found by replacing one of the $q_{2\mu}$ operators by its average value. We have

$$V_{qq}^\tau = \sqrt{6} \sum_{\mu} (-1)^\mu Z_{2-\mu}^{\tau+} q_{2\mu}. \quad (13)$$

Here

$$\begin{aligned} Z_{2\mu}^{n+} &= \kappa R_{2\mu}^{n+} + \bar{\kappa} R_{2\mu}^{p+}, \quad Z_{2\mu}^{p+} = \kappa R_{2\mu}^{p+} + \bar{\kappa} R_{2\mu}^{n+}, \\ R_{2\mu}^{\tau+}(t) &= \frac{1}{\sqrt{6}} \int d(\mathbf{p}, \mathbf{r}) q_{2\mu}(\mathbf{r}) f^{\tau+}(\mathbf{r}, \mathbf{p}, t) \end{aligned} \quad (14)$$

with $\int d(\mathbf{p}, \mathbf{r}) \equiv (2\pi\hbar)^{-3} \int d^3 p \int d^3 r$ and τ being the isospin index.

3. Spin-spin interaction

The analogous expression for H_{ss} is found in a standard way [11] with the following result for the Wigner transform of the proton mean field:

$$\begin{aligned} V_p^{ss'}(\mathbf{r}, t) &= 3\chi \frac{\hbar^2}{8} \left[\delta_{s\downarrow} \delta_{s'\uparrow} n_p^{\uparrow\uparrow} + \delta_{s\uparrow} \delta_{s'\downarrow} n_p^{\downarrow\downarrow} \right. \\ &- \left. \delta_{s\downarrow} \delta_{s'\downarrow} n_p^{\uparrow\uparrow} - \delta_{s\uparrow} \delta_{s'\uparrow} n_p^{\downarrow\downarrow} \right] \\ &+ \bar{\chi} \frac{\hbar^2}{8} \left[2\delta_{s\downarrow} \delta_{s'\uparrow} n_n^{\uparrow\uparrow} + 2\delta_{s\uparrow} \delta_{s'\downarrow} n_n^{\downarrow\downarrow} \right. \\ &+ \left. (\delta_{s\uparrow} \delta_{s'\uparrow} - \delta_{s\downarrow} \delta_{s'\downarrow}) (n_n^{\uparrow\uparrow} - n_n^{\downarrow\downarrow}) \right], \end{aligned} \quad (15)$$

where $n_{\tau}^{ss'}(\mathbf{r}, t) = \int \frac{d\mathbf{p}}{(2\pi\hbar)^3} f_{\tau}^{ss'}(\mathbf{r}, \mathbf{p}, t)$. The Wigner transform of the neutron mean field $V_n^{ss'}$ is obtained from (15) by the obvious change of indices $\mathbf{p} \leftrightarrow \mathbf{n}$.

B. Pair potential

The Wigner transform of the pair potential (pairing gap) $\Delta^{\tau}(\mathbf{r}, \mathbf{p})$ is related to the Wigner transform of the anomalous density by [9]

$$\Delta^{\tau}(\mathbf{r}, \mathbf{p}) = - \int \frac{d\mathbf{p}'}{(2\pi\hbar)^3} v(|\mathbf{p} - \mathbf{p}'|) \kappa^{\tau}(\mathbf{r}, \mathbf{p}'), \quad (16)$$

where $v(p)$ is a Fourier transform of the two-body interaction. We take for the pairing interaction a simple Gaussian of strength V_0 and range r_p [9]

$$v(p) = \beta e^{-\alpha p^2}, \quad (17)$$

with $\beta = -|V_0|(r_p\sqrt{\pi})^3$ and $\alpha = r_p^2/4\hbar^2$. The following values of parameters were used in calculations: $V_0^p = 27$ MeV, $V_0^n = 23$ MeV, $r_p^p = 1.50$ fm, $r_p^n = 1.85$ fm for nuclei with $A = 150 - 186$ and $V_0^p = 25.5$ MeV, $V_0^n = 21.5$ MeV, $r_p^p = 1.5$ fm, $r_p^n = 1.80$ fm for Actinides. Exceptions are listed in the captions to the corresponding Tables.

IV. EQUATIONS OF MOTION

Equations (5) will be solved by the method of moments in a small amplitude approximation. To this end all functions $f(\mathbf{r}, \mathbf{p}, t)$ and $\kappa(\mathbf{r}, \mathbf{p}, t)$ are divided into an equilibrium part and a variation: $f(\mathbf{r}, \mathbf{p}, t) = f(\mathbf{r}, \mathbf{p})_{\text{eq}} + \delta f(\mathbf{r}, \mathbf{p}, t)$, $\kappa(\mathbf{r}, \mathbf{p}, t) = \kappa(\mathbf{r}, \mathbf{p})_{\text{eq}} + \delta\kappa(\mathbf{r}, \mathbf{p}, t)$. Then the equations are linearized neglecting terms quadratic in the variations.

After linearization, the phase of Δ (and of κ) is expressed by $\delta\Delta^i$ (and $\delta\kappa^i$), while $\delta\Delta^r$ (and $\delta\kappa^r$) describes oscillations of the magnitude of Δ (and of κ). From general arguments one can expect that the phase of Δ (and of κ , since both are linked, according to equation (16)) is much more relevant than its magnitude, since the former determines the superfluid velocity. Let us therefore assume that

$$\delta\kappa^r(\mathbf{r}, \mathbf{p}) \ll \delta\kappa^i(\mathbf{r}, \mathbf{p}). \quad (18)$$

This assumption was explicitly confirmed in [12] for the case of superfluid trapped fermionic atoms, where it was shown that $\delta\Delta^r$ is suppressed with respect to $\delta\Delta^i$ by one order of Δ/E_F , where E_F denotes the Fermi energy. The assumption (18) allows one to neglect all terms containing the variations $\delta\kappa^r$ and $\delta\Delta^r$ in the equations (5) after their linearization.

Integrating these equations over phase space with the weights

$$W = \{r \otimes p\}_{\lambda\mu}, \{r \otimes r\}_{\lambda\mu}, \{p \otimes p\}_{\lambda\mu}, \text{ and } 1$$

one gets dynamic equations for the following collective variables:

$$\begin{aligned} \mathcal{L}_{\lambda\mu}^{\tau\zeta}(t) &= \int d(\mathbf{p}, \mathbf{r}) \{r \otimes p\}_{\lambda\mu} \delta f_o^{\tau\zeta}(\mathbf{r}, \mathbf{p}, t), \\ \mathcal{R}_{\lambda\mu}^{\tau\zeta}(t) &= \int d(\mathbf{p}, \mathbf{r}) \{r \otimes r\}_{\lambda\mu} \delta f_e^{\tau\zeta}(\mathbf{r}, \mathbf{p}, t), \\ \mathcal{P}_{\lambda\mu}^{\tau\zeta}(t) &= \int d(\mathbf{p}, \mathbf{r}) \{p \otimes p\}_{\lambda\mu} \delta f_e^{\tau\zeta}(\mathbf{r}, \mathbf{p}, t), \\ \mathcal{F}^{\tau\zeta}(t) &= \int d(\mathbf{p}, \mathbf{r}) \delta f_e^{\tau\zeta}(\mathbf{r}, \mathbf{p}, t), \\ \tilde{\mathcal{L}}_{\lambda\mu}^{\tau}(t) &= \int d(\mathbf{p}, \mathbf{r}) \{r \otimes p\}_{\lambda\mu} \delta \kappa_o^{\tau i}(\mathbf{r}, \mathbf{p}, t), \\ \tilde{\mathcal{R}}_{\lambda\mu}^{\tau}(t) &= \int d(\mathbf{p}, \mathbf{r}) \{r \otimes r\}_{\lambda\mu} \delta \kappa_e^{\tau i}(\mathbf{r}, \mathbf{p}, t), \\ \tilde{\mathcal{P}}_{\lambda\mu}^{\tau}(t) &= \int d(\mathbf{p}, \mathbf{r}) \{p \otimes p\}_{\lambda\mu} \delta \kappa_e^{\tau i}(\mathbf{r}, \mathbf{p}, t), \end{aligned}$$

where $\zeta = +, -, \uparrow\downarrow, \downarrow\uparrow$,

The required expressions for h^{\pm} , $h^{\uparrow\downarrow}$ and $h^{\downarrow\uparrow}$ are

$$\begin{aligned} h_{\tau}^{\pm} &= \frac{p^2}{m} + m\omega^2 r^2 + 12 \sum_{\mu} (-1)^{\mu} Z_{2\mu}^{\tau\pm}(t) \{r \otimes r\}_{2-\mu} \\ &+ V_{\tau}^{\pm}(\mathbf{r}, t) - \mu^{\tau}, \end{aligned}$$

μ^{τ} being the chemical potential of protons ($\tau = p$) or neutrons ($\tau = n$),

$$\begin{aligned} h_{\tau}^{-} &= -\hbar\eta l_0 + V_{\tau}^{-}(\mathbf{r}, t), \\ h_{\tau}^{\uparrow\downarrow} &= -\frac{\hbar}{\sqrt{2}}\eta l_{-1} + V_{\tau}^{\uparrow\downarrow}(\mathbf{r}, t), \\ h_{\tau}^{\downarrow\uparrow} &= \frac{\hbar}{\sqrt{2}}\eta l_1 + V_{\tau}^{\downarrow\uparrow}(\mathbf{r}, t), \end{aligned}$$

where according to (15)

$$\begin{aligned} V_p^+(\mathbf{r}, t) &= -3\frac{\hbar^2}{8}\chi n_p^+(\mathbf{r}, t), \\ V_p^-(\mathbf{r}, t) &= 3\frac{\hbar^2}{8}\chi n_p^-(\mathbf{r}, t) + \frac{\hbar^2}{4}\bar{\chi} n_n^-(\mathbf{r}, t), \\ V_p^{\uparrow\downarrow}(\mathbf{r}, t) &= 3\frac{\hbar^2}{8}\chi n_p^{\uparrow\downarrow}(\mathbf{r}, t) + \frac{\hbar^2}{4}\bar{\chi} n_n^{\uparrow\downarrow}(\mathbf{r}, t), \\ V_p^{\downarrow\uparrow}(\mathbf{r}, t) &= 3\frac{\hbar^2}{8}\chi n_p^{\downarrow\uparrow}(\mathbf{r}, t) + \frac{\hbar^2}{4}\bar{\chi} n_n^{\downarrow\uparrow}(\mathbf{r}, t) \quad (19) \end{aligned}$$

and the neutron potentials V_n^{ζ} are obtained by the obvious change of indices $\mathbf{p} \leftrightarrow \mathbf{n}$. Variations of these mean fields read:

$$\delta h_{\tau}^{\pm} = 12 \sum_{\mu} (-1)^{\mu} \delta Z_{2\mu}^{\tau\pm}(t) \{r \otimes r\}_{2-\mu} + \delta V_{\tau}^{\pm}(\mathbf{r}, t),$$

where $\delta Z_{2\mu}^{\text{p}+} = \kappa \delta R_{2\mu}^{\text{p}+} + \bar{\kappa} \delta R_{2\mu}^{\text{n}+}$, $\delta R_{\lambda\mu}^{\tau+}(t) \equiv \mathcal{R}_{\lambda\mu}^{\tau+}(t)$ and

$$\begin{aligned}\delta V_{\text{p}}^+(\mathbf{r}, t) &= -3 \frac{\hbar^2}{8} \chi \delta n_{\text{p}}^+(\mathbf{r}, t), \\ \delta n_{\text{p}}^+(\mathbf{r}, t) &= \int \frac{d^3 p}{(2\pi\hbar)^3} \delta f_{\text{p}}^+(\mathbf{r}, \mathbf{p}, t).\end{aligned}$$

Variations of h^- , $h^{\uparrow\downarrow}$ and $h^{\downarrow\uparrow}$ are obtained in a similar way. The detailed procedure of the density variation is described in Appendix B of [11]. Variation of the pair potential is

$$\delta \Delta^\tau(\mathbf{r}, \mathbf{p}, t) = - \int \frac{d\mathbf{p}'}{(2\pi\hbar)^3} v(|\mathbf{p} - \mathbf{p}'|) \delta \kappa^\tau(\mathbf{r}, \mathbf{p}', t). \quad (20)$$

We are interested in the scissors mode with quantum number $K^\pi = 1^+$. Therefore, we only need the

part of dynamic equations with $\mu = 1$.

It is convenient to rewrite the dynamical equations for neutron and proton variables in terms of isoscalar and isovector variables

$$\begin{aligned}\mathcal{R}_{\lambda\mu} &= \mathcal{R}_{\lambda\mu}^{\text{n}} + \mathcal{R}_{\lambda\mu}^{\text{p}}, & \bar{\mathcal{R}}_{\lambda\mu} &= \mathcal{R}_{\lambda\mu}^{\text{n}} - \mathcal{R}_{\lambda\mu}^{\text{p}}, \\ \mathcal{P}_{\lambda\mu} &= \mathcal{P}_{\lambda\mu}^{\text{n}} + \mathcal{P}_{\lambda\mu}^{\text{p}}, & \bar{\mathcal{P}}_{\lambda\mu} &= \mathcal{P}_{\lambda\mu}^{\text{n}} - \mathcal{P}_{\lambda\mu}^{\text{p}}, \\ \mathcal{L}_{\lambda\mu} &= \mathcal{L}_{\lambda\mu}^{\text{n}} + \mathcal{L}_{\lambda\mu}^{\text{p}}, & \bar{\mathcal{L}}_{\lambda\mu} &= \mathcal{L}_{\lambda\mu}^{\text{n}} - \mathcal{L}_{\lambda\mu}^{\text{p}}, \\ \mathcal{F} &= \mathcal{F}^{\text{n}} + \mathcal{F}^{\text{p}}, & \bar{\mathcal{F}} &= \mathcal{F}^{\text{n}} - \mathcal{F}^{\text{p}}.\end{aligned} \quad (21)$$

We also define isovector and isoscalar strength constants $\kappa_1 = \frac{1}{2}(\kappa - \bar{\kappa})$ and $\kappa_0 = \frac{1}{2}(\kappa + \bar{\kappa})$ connected by the relation $\kappa_1 = \alpha \kappa_0$ with $\alpha = -2$ [4].

The integration yields the following set of equations for isovector variables:

$$\begin{aligned}\dot{\mathcal{L}}_{21}^+ &= \frac{1}{m} \bar{\mathcal{P}}_{21}^+ - [m\omega^2 + \kappa_0(4\alpha Q_{00} + (1+\alpha)Q_{20})] \bar{\mathcal{R}}_{21}^+ - i\hbar \frac{\eta}{2} [\bar{\mathcal{L}}_{21}^- + 2\bar{\mathcal{L}}_{22}^{\uparrow\downarrow} + \sqrt{6}\bar{\mathcal{L}}_{20}^{\downarrow\uparrow}] \\ &\quad - \underbrace{\kappa_0(4\bar{Q}_{00} + (1+\alpha)\bar{Q}_{20})}_{\text{coupling term}} \mathcal{R}_{21}^+, \\ \dot{\mathcal{L}}_{21}^- &= \frac{1}{m} \bar{\mathcal{P}}_{21}^- - \left[m\omega^2 + \kappa_0 Q_{20} - \frac{\hbar^2}{15} (3\chi - \bar{\chi}) \frac{I_1}{A_1 A_2} (Q_{00} + Q_{20}/4) \right] \bar{\mathcal{R}}_{21}^- - i\hbar \frac{\eta}{2} \bar{\mathcal{L}}_{21}^+ + \frac{4}{\hbar} I_{rp}^{\kappa\Delta}(r') \bar{\mathcal{L}}_{21} \\ &\quad - \left[\alpha \kappa_0 \bar{Q}_{20} - \frac{\hbar^2}{15} (3\chi + \bar{\chi}) \frac{I_1}{A_1 A_2} (\bar{Q}_{00} + \bar{Q}_{20}/4) \right] \mathcal{R}_{21}^- + \frac{4}{\hbar} \bar{I}_{rp}^{\kappa\Delta}(r') \tilde{\mathcal{L}}_{21}, \\ \dot{\mathcal{L}}_{22}^{\uparrow\downarrow} &= \frac{1}{m} \bar{\mathcal{P}}_{22}^{\uparrow\downarrow} - \left[m\omega^2 - 2\kappa_0 Q_{20} - 4\hbar^2 (3\chi - \bar{\chi}) \frac{I_1}{A_1 A_2} (Q_{20} + Q_{00}) \right] \bar{\mathcal{R}}_{22}^{\uparrow\downarrow} - i\hbar \frac{\eta}{2} \bar{\mathcal{L}}_{21}^+ \\ &\quad + \left[2\alpha \kappa_0 \bar{Q}_{20} + 4\hbar^2 (3\chi + \bar{\chi}) \frac{I_1}{A_1 A_2} (\bar{Q}_{20} + \bar{Q}_{00}) \right] \mathcal{R}_{22}^{\uparrow\downarrow}, \\ \dot{\mathcal{L}}_{20}^{\downarrow\uparrow} &= \frac{1}{m} \bar{\mathcal{P}}_{20}^{\downarrow\uparrow} - [m\omega^2 + 2\kappa_0 Q_{20}] \bar{\mathcal{R}}_{20}^{\downarrow\uparrow} + 2\sqrt{2}\kappa_0 Q_{20} \bar{\mathcal{R}}_{00}^{\downarrow\uparrow} - i\hbar \frac{\eta}{2} \sqrt{\frac{3}{2}} \bar{\mathcal{L}}_{21}^+ \\ &\quad + \frac{\hbar^2}{15} (3\chi - \bar{\chi}) \frac{I_1}{A_1 A_2} [Q_{00} \bar{\mathcal{R}}_{20}^{\downarrow\uparrow} + Q_{20} \bar{\mathcal{R}}_{00}^{\downarrow\uparrow} / \sqrt{2}], \\ &\quad - 2\alpha \kappa_0 \bar{Q}_{20} [\mathcal{R}_{20}^{\downarrow\uparrow} + \sqrt{2} \mathcal{R}_{00}^{\downarrow\uparrow}] + \frac{\hbar^2}{15} (3\chi + \bar{\chi}) \frac{I_1}{A_1 A_2} [\bar{Q}_{00} \mathcal{R}_{20}^{\downarrow\uparrow} + \bar{Q}_{20} \mathcal{R}_{00}^{\downarrow\uparrow} / \sqrt{2}], \\ \dot{\mathcal{L}}_{11}^+ &= -3(1-\alpha)\kappa_0 Q_{20} \bar{\mathcal{R}}_{21}^+ - i\hbar \frac{\eta}{2} [\bar{\mathcal{L}}_{11}^- + \sqrt{2}\bar{\mathcal{L}}_{10}^{\downarrow\uparrow}] + \underbrace{3(1-\alpha)\kappa_0 \bar{Q}_{20}}_{\text{coupling term}} \mathcal{R}_{21}^+, \\ \dot{\mathcal{L}}_{11}^- &= - \left[3\kappa_0 Q_{20} + \frac{\hbar^2}{20} (3\chi - \bar{\chi}) \frac{I_1}{A_1 A_2} Q_{20} \right] \bar{\mathcal{R}}_{21}^- + \frac{4}{\hbar} I_{rp}^{\kappa\Delta}(r') \bar{\mathcal{L}}_{11} - \hbar \frac{\eta}{2} [i\bar{\mathcal{L}}_{11}^+ + \hbar \bar{\mathcal{F}}^{\downarrow\uparrow}] \\ &\quad - \left[3\alpha \kappa_0 \bar{Q}_{20} + \frac{\hbar^2}{20} (3\chi + \bar{\chi}) \frac{I_1}{A_1 A_2} \bar{Q}_{20} \right] \mathcal{R}_{21}^- + \frac{4}{\hbar} \bar{I}_{rp}^{\kappa\Delta}(r') \tilde{\mathcal{L}}_{11}, \\ \dot{\mathcal{L}}_{10}^{\downarrow\uparrow} &= -\hbar \frac{\eta}{2\sqrt{2}} [i\bar{\mathcal{L}}_{11}^+ + \hbar \bar{\mathcal{F}}^{\downarrow\uparrow}], \\ \dot{\mathcal{F}}^{\downarrow\uparrow} &= -\eta [\bar{\mathcal{L}}_{11}^- + \sqrt{2}\bar{\mathcal{L}}_{10}^{\downarrow\uparrow}],\end{aligned}$$

$$\begin{aligned}
\dot{\bar{\mathcal{R}}}_{21}^+ &= \frac{2}{m} \bar{\mathcal{L}}_{21}^+ - i\hbar \frac{\eta}{2} \left[\bar{\mathcal{R}}_{21}^- + 2\bar{\mathcal{R}}_{22}^{\uparrow\downarrow} + \sqrt{6}\bar{\mathcal{R}}_{20}^{\uparrow\downarrow} \right], \\
\dot{\bar{\mathcal{R}}}_{21}^- &= \frac{2}{m} \bar{\mathcal{L}}_{21}^- - i\hbar \frac{\eta}{2} \bar{\mathcal{R}}_{21}^+, \\
\dot{\bar{\mathcal{R}}}_{22}^{\uparrow\downarrow} &= \frac{2}{m} \bar{\mathcal{L}}_{22}^{\uparrow\downarrow} - i\hbar \frac{\eta}{2} \bar{\mathcal{R}}_{21}^+, \\
\dot{\bar{\mathcal{R}}}_{20}^{\uparrow\downarrow} &= \frac{2}{m} \bar{\mathcal{L}}_{20}^{\uparrow\downarrow} - i\hbar \frac{\eta}{2} \sqrt{\frac{3}{2}} \bar{\mathcal{R}}_{21}^+, \\
\dot{\bar{\mathcal{P}}}_{21}^+ &= -2 \left[m\omega^2 + \kappa_0 Q_{20} \right] \bar{\mathcal{L}}_{21}^+ + 6\kappa_0 Q_{20} \bar{\mathcal{L}}_{11}^+ - i\hbar \frac{\eta}{2} \left[\bar{\mathcal{P}}_{21}^- + 2\bar{\mathcal{P}}_{22}^{\uparrow\downarrow} + \sqrt{6}\bar{\mathcal{P}}_{20}^{\uparrow\downarrow} \right] \\
&\quad + \frac{3}{8} \hbar^2 \chi \frac{I_2}{A_1 A_2} \left[(Q_{20} + 4Q_{00}) \bar{\mathcal{L}}_{21}^+ + 3Q_{20} \bar{\mathcal{L}}_{11}^+ \right] + \frac{4}{\hbar} |V_0| I_{pp}^{\kappa\Delta}(r') \bar{\bar{\mathcal{P}}}_{21} \\
&\quad + \underbrace{2\alpha\kappa_0 \bar{Q}_{20} (3\mathcal{L}_{11}^+ - \mathcal{L}_{21}^+) + \frac{3}{8} \hbar^2 \chi \frac{I_2}{A_1 A_2} \left[(\bar{Q}_{20} + 4\bar{Q}_{00}) \mathcal{L}_{21}^+ + 3\bar{Q}_{20} \mathcal{L}_{11}^+ \right]}_{\text{}} + \frac{4}{\hbar} |V_0| \bar{I}_{pp}^{\kappa\Delta}(r') \bar{\tilde{\mathcal{P}}}_{21}, \\
\dot{\bar{\mathcal{P}}}_{21}^- &= -2 \left[m\omega^2 + \kappa_0 Q_{20} \right] \bar{\mathcal{L}}_{21}^- + 6\kappa_0 Q_{20} \bar{\mathcal{L}}_{11}^- - 6\sqrt{2}\alpha\kappa_0 L_{10}^-(\text{eq}) \bar{\mathcal{R}}_{21}^+ - i\hbar \frac{\eta}{2} \bar{\mathcal{P}}_{21}^+ \\
&\quad + \frac{3}{8} \hbar^2 \chi \frac{I_2}{A_1 A_2} \left[(Q_{20} + 4Q_{00}) \bar{\mathcal{L}}_{21}^- + 3Q_{20} \bar{\mathcal{L}}_{11}^- \right] \\
&\quad + \underbrace{2\alpha\kappa_0 \bar{Q}_{20} (3\mathcal{L}_{11}^- - \mathcal{L}_{21}^-) + \frac{3}{8} \hbar^2 \chi \frac{I_2}{A_1 A_2} \left[(\bar{Q}_{20} + 4\bar{Q}_{00}) \mathcal{L}_{21}^- + 3\bar{Q}_{20} \mathcal{L}_{11}^- \right]}_{\text{}} - 6\sqrt{2}\kappa_0 \bar{L}_{10}^-(\text{eq}) \bar{\mathcal{R}}_{21}^+, \\
\dot{\bar{\mathcal{P}}}_{22}^{\uparrow\downarrow} &= -2 \left[m\omega^2 - 2\kappa_0 Q_{20} \right] \bar{\mathcal{L}}_{22}^{\uparrow\downarrow} - i\hbar \frac{\eta}{2} \bar{\mathcal{P}}_{21}^+ + \frac{3}{2} \hbar^2 \chi \frac{I_2}{A_1 A_2} (Q_{20} + Q_{00}) \bar{\mathcal{L}}_{22}^{\uparrow\downarrow} \\
&\quad + \underbrace{4\alpha\kappa_0 \bar{Q}_{20} \mathcal{L}_{22}^{\uparrow\downarrow} + \frac{3}{2} \hbar^2 \chi \frac{I_2}{A_1 A_2} (Q_{20} + Q_{00}) \mathcal{L}_{22}^{\uparrow\downarrow}}_{\text{}}, \\
\dot{\bar{\mathcal{P}}}_{20}^{\uparrow\downarrow} &= -2 \left[m\omega^2 + 2\kappa_0 Q_{20} \right] \bar{\mathcal{L}}_{20}^{\uparrow\downarrow} + 4\sqrt{2}\kappa_0 Q_{20} \bar{\mathcal{L}}_{00}^{\uparrow\downarrow} - i\hbar \frac{\eta}{2} \sqrt{\frac{3}{2}} \bar{\mathcal{P}}_{21}^+ + \frac{3}{2} \hbar^2 \chi \frac{I_2}{A_1 A_2} \left[Q_{00} \bar{\mathcal{L}}_{20}^{\uparrow\downarrow} + Q_{20} \bar{\mathcal{L}}_{00}^{\uparrow\downarrow} / \sqrt{2} \right] \\
&\quad + \underbrace{4\alpha\kappa_0 \bar{Q}_{20} \left(\sqrt{2} \mathcal{L}_{00}^{\uparrow\downarrow} - \mathcal{L}_{20}^{\uparrow\downarrow} \right) + \frac{3}{2} \hbar^2 \chi \frac{I_2}{A_1 A_2} \left[\bar{Q}_{00} \mathcal{L}_{20}^{\uparrow\downarrow} + \bar{Q}_{20} \mathcal{L}_{00}^{\uparrow\downarrow} / \sqrt{2} \right]}_{\text{}}, \\
\dot{\bar{\mathcal{L}}}_{00}^{\uparrow\downarrow} &= \frac{1}{m} \bar{\mathcal{P}}_{00}^{\uparrow\downarrow} - m\omega^2 \bar{\mathcal{R}}_{00}^{\uparrow\downarrow} + 2\sqrt{2}\kappa_0 Q_{20} \bar{\mathcal{R}}_{20}^{\uparrow\downarrow} + \frac{\hbar^2}{4 A_1 A_2} \left[\left(\chi - \frac{\bar{\chi}}{3} \right) I_1 - \frac{9}{4} \chi I_2 \right] \left[(2Q_{00} + Q_{20}) \bar{\mathcal{R}}_{00}^{\uparrow\downarrow} + \sqrt{2} Q_{20} \bar{\mathcal{R}}_{20}^{\uparrow\downarrow} \right] \\
&\quad + \underbrace{2\sqrt{2}\alpha\kappa_0 \bar{Q}_{20} \mathcal{R}_{20}^{\uparrow\downarrow} + \frac{\hbar^2}{4 A_1 A_2} \left[\left(\chi + \frac{\bar{\chi}}{3} \right) I_1 - \frac{9}{4} \chi I_2 \right] \left[(2\bar{Q}_{00} + \bar{Q}_{20}) \mathcal{R}_{00}^{\uparrow\downarrow} + \sqrt{2} \bar{Q}_{20} \mathcal{R}_{20}^{\uparrow\downarrow} \right]}_{\text{}}, \\
\dot{\bar{\mathcal{R}}}_{00}^{\uparrow\downarrow} &= \frac{2}{m} \bar{\mathcal{L}}_{00}^{\uparrow\downarrow}, \\
\dot{\bar{\mathcal{P}}}_{00}^{\uparrow\downarrow} &= -2m\omega^2 \bar{\mathcal{L}}_{00}^{\uparrow\downarrow} + 4\sqrt{2}\kappa_0 Q_{20} \bar{\mathcal{L}}_{20}^{\uparrow\downarrow} + \frac{3}{4} \hbar^2 \chi \frac{I_2}{A_1 A_2} \left[(2Q_{00} + Q_{20}) \bar{\mathcal{L}}_{00}^{\uparrow\downarrow} + \sqrt{2} Q_{20} \bar{\mathcal{L}}_{20}^{\uparrow\downarrow} \right] \\
&\quad + \underbrace{4\sqrt{2}\alpha\kappa_0 \bar{Q}_{20} \mathcal{L}_{20}^{\uparrow\downarrow} + \frac{3}{4} \hbar^2 \chi \frac{I_2}{A_1 A_2} \left[(2\bar{Q}_{00} + \bar{Q}_{20}) \mathcal{L}_{00}^{\uparrow\downarrow} + \sqrt{2} \bar{Q}_{20} \mathcal{L}_{20}^{\uparrow\downarrow} \right]}_{\text{}}, \\
\dot{\bar{\mathcal{P}}}_{21}^- &= -\frac{1}{\hbar} \Delta(r') \bar{\mathcal{P}}_{21}^+ + 6\hbar\alpha\kappa_0 K_0 \bar{\mathcal{R}}_{21}^+ - \underbrace{\frac{1}{\hbar} \bar{\Delta}(r') \mathcal{P}_{21}^+ + 6\hbar\kappa_0 \bar{K}_0 \mathcal{R}_{21}^+}_{\text{}}, \\
\dot{\bar{\mathcal{L}}}_{21}^- &= -\frac{1}{\hbar} \Delta(r') \bar{\mathcal{L}}_{21}^- - \underbrace{\frac{1}{\hbar} \bar{\Delta}(r') \mathcal{L}_{21}^-}_{\text{}}, \\
\dot{\bar{\mathcal{L}}}_{11}^- &= -\frac{1}{\hbar} \Delta(r') \bar{\mathcal{L}}_{11}^- - \underbrace{\frac{1}{\hbar} \bar{\Delta}(r') \mathcal{L}_{11}^-}_{\text{}}, \tag{22}
\end{aligned}$$

The set of equations for isoscalar variables reads:

$$\begin{aligned}
\dot{\mathcal{L}}_{21}^+ &= \frac{1}{m} \mathcal{P}_{21}^+ - [m\omega^2 + 2\kappa_0(2Q_{00} + Q_{20})] \mathcal{R}_{21}^+ - i\hbar \frac{\eta}{2} \left[\mathcal{L}_{21}^- + 2\mathcal{L}_{22}^{\uparrow\downarrow} + \sqrt{6}\mathcal{L}_{20}^{\downarrow\uparrow} \right] \\
&\quad - \underbrace{\alpha\kappa_0(2\bar{Q}_{00} + \bar{Q}_{20}) \bar{\mathcal{R}}_{21}^+}_{\text{coupling term}}, \\
\dot{\mathcal{L}}_{21}^- &= \frac{1}{m} \mathcal{P}_{21}^- - \left[m\omega^2 + \kappa_0 Q_{20} - \frac{\hbar^2}{15} (3\chi + \bar{\chi}) \frac{I_1}{A_1 A_2} (Q_{00} + Q_{20}/4) \right] \mathcal{R}_{21}^- - i\hbar \frac{\eta}{2} \mathcal{L}_{21}^+ + \frac{4}{\hbar} I_{rp}^{\kappa\Delta}(r') \tilde{\mathcal{L}}_{21} \\
&\quad - \underbrace{\left[\alpha\kappa_0 \bar{Q}_{20} - \frac{\hbar^2}{15} (3\chi - \bar{\chi}) \frac{I_1}{A_1 A_2} (\bar{Q}_{00} + \bar{Q}_{20}/4) \right] \bar{\mathcal{R}}_{21}^- + \frac{4}{\hbar} \bar{I}_{rp}^{\kappa\Delta}(r') \bar{\tilde{\mathcal{L}}}_{21}}_{}, \\
\dot{\mathcal{L}}_{22}^{\uparrow\downarrow} &= \frac{1}{m} \mathcal{P}_{22}^{\uparrow\downarrow} - \left[m\omega^2 - 2\kappa_0 Q_{20} - 4\hbar^2 (3\chi + \bar{\chi}) \frac{I_1}{A_1 A_2} (Q_{20} + Q_{00}) \right] \mathcal{R}_{22}^{\uparrow\downarrow} - i\hbar \frac{\eta}{2} \mathcal{L}_{21}^+ \\
&\quad + \underbrace{\left[2\alpha\kappa_0 \bar{Q}_{20} + 4\hbar^2 (3\chi - \bar{\chi}) \frac{I_1}{A_1 A_2} (\bar{Q}_{20} + \bar{Q}_{00}) \right] \bar{\mathcal{R}}_{22}^{\uparrow\downarrow}}_{}, \\
\dot{\mathcal{L}}_{20}^{\downarrow\uparrow} &= \frac{1}{m} \mathcal{P}_{20}^{\downarrow\uparrow} - [m\omega^2 + 2\kappa_0 Q_{20}] \mathcal{R}_{20}^{\downarrow\uparrow} + 2\sqrt{2}\kappa_0 Q_{20} \mathcal{R}_{00}^{\downarrow\uparrow} - i\hbar \frac{\eta}{2} \sqrt{\frac{3}{2}} \mathcal{L}_{21}^+ \\
&\quad + \frac{\hbar^2}{15} (3\chi + \bar{\chi}) \frac{I_1}{A_1 A_2} \left[Q_{00} \mathcal{R}_{20}^{\downarrow\uparrow} + Q_{20} \mathcal{R}_{00}^{\downarrow\uparrow} / \sqrt{2} \right], \\
&\quad - \underbrace{2\alpha\kappa_0 \bar{Q}_{20} \left[\bar{\mathcal{R}}_{20}^{\downarrow\uparrow} + \sqrt{2} \bar{\mathcal{R}}_{00}^{\downarrow\uparrow} \right] + \frac{\hbar^2}{15} (3\chi - \bar{\chi}) \frac{I_1}{A_1 A_2} \left[\bar{Q}_{00} \bar{\mathcal{R}}_{20}^{\downarrow\uparrow} + \bar{Q}_{20} \bar{\mathcal{R}}_{00}^{\downarrow\uparrow} / \sqrt{2} \right]}_{}, \\
\dot{\mathcal{L}}_{11}^+ &= -i\hbar \frac{\eta}{2} \left[\mathcal{L}_{11}^- + \sqrt{2}\mathcal{L}_{10}^{\downarrow\uparrow} \right], \\
\dot{\mathcal{L}}_{11}^- &= - \left[3\kappa_0 Q_{20} + \frac{\hbar^2}{20} (3\chi + \bar{\chi}) \frac{I_1}{A_1 A_2} Q_{20} \right] \mathcal{R}_{21}^- + \frac{4}{\hbar} I_{rp}^{\kappa\Delta}(r') \tilde{\mathcal{L}}_{11} - \hbar \frac{\eta}{2} [i\mathcal{L}_{11}^+ + \hbar\mathcal{F}^{\downarrow\uparrow}] \\
&\quad - \underbrace{\left[3\alpha\kappa_0 \bar{Q}_{20} + \frac{\hbar^2}{20} (3\chi - \bar{\chi}) \frac{I_1}{A_1 A_2} \bar{Q}_{20} \right] \bar{\mathcal{R}}_{21}^- + \frac{4}{\hbar} \bar{I}_{rp}^{\kappa\Delta}(r') \bar{\tilde{\mathcal{L}}}_{11}}_{}, \\
\dot{\mathcal{L}}_{10}^{\downarrow\uparrow} &= -\hbar \frac{\eta}{2\sqrt{2}} [i\mathcal{L}_{11}^+ + \hbar\mathcal{F}^{\downarrow\uparrow}], \\
\dot{\mathcal{F}}^{\downarrow\uparrow} &= -\eta \left[\mathcal{L}_{11}^- + \sqrt{2}\mathcal{L}_{10}^{\downarrow\uparrow} \right], \\
\dot{\mathcal{R}}_{21}^+ &= \frac{2}{m} \mathcal{L}_{21}^+ - i\hbar \frac{\eta}{2} \left[\mathcal{R}_{21}^- + 2\mathcal{R}_{22}^{\uparrow\downarrow} + \sqrt{6}\mathcal{R}_{20}^{\downarrow\uparrow} \right], \\
\dot{\mathcal{R}}_{21}^- &= \frac{2}{m} \mathcal{L}_{21}^- - i\hbar \frac{\eta}{2} \mathcal{R}_{21}^+, \\
\dot{\mathcal{R}}_{22}^{\uparrow\downarrow} &= \frac{2}{m} \mathcal{L}_{22}^{\uparrow\downarrow} - i\hbar \frac{\eta}{2} \mathcal{R}_{21}^+, \\
\dot{\mathcal{R}}_{20}^{\downarrow\uparrow} &= \frac{2}{m} \mathcal{L}_{20}^{\downarrow\uparrow} - i\hbar \frac{\eta}{2} \sqrt{\frac{3}{2}} \mathcal{R}_{21}^+, \\
\dot{\mathcal{P}}_{21}^+ &= -2 [m\omega^2 + \kappa_0 Q_{20}] \mathcal{L}_{21}^+ + 6\kappa_0 Q_{20} \mathcal{L}_{11}^+ - i\hbar \frac{\eta}{2} \left[\mathcal{P}_{21}^- + 2\mathcal{P}_{22}^{\uparrow\downarrow} + \sqrt{6}\mathcal{P}_{20}^{\downarrow\uparrow} \right] \\
&\quad + \frac{3}{8} \hbar^2 \chi \frac{I_2}{A_1 A_2} \left[(Q_{20} + 4Q_{00}) \mathcal{L}_{21}^+ + 3Q_{20} \mathcal{L}_{11}^+ \right] + \frac{4}{\hbar} |V_0| I_{pp}^{\kappa\Delta}(r') \bar{\mathcal{P}}_{21} \\
&\quad + \underbrace{2\alpha\kappa_0 \bar{Q}_{20} (3\bar{\mathcal{L}}_{11}^+ - \bar{\mathcal{L}}_{21}^+) + \frac{3}{8} \hbar^2 \chi \frac{I_2}{A_1 A_2} \left[(\bar{Q}_{20} + 4\bar{Q}_{00}) \bar{\mathcal{L}}_{21}^+ + 3\bar{Q}_{20} \bar{\mathcal{L}}_{11}^+ \right] + \frac{4}{\hbar} |V_0| \bar{I}_{pp}^{\kappa\Delta}(r') \bar{\mathcal{P}}_{21}}_{}, \\
\dot{\mathcal{P}}_{21}^- &= -2 [m\omega^2 + \kappa_0 Q_{20}] \mathcal{L}_{21}^- + 6\kappa_0 Q_{20} \mathcal{L}_{11}^- - 6\sqrt{2}\kappa_0 L_{10}^-(\text{eq}) \mathcal{R}_{21}^+ - i\hbar \frac{\eta}{2} \mathcal{P}_{21}^+ \\
&\quad + \frac{3}{8} \hbar^2 \chi \frac{I_2}{A_1 A_2} \left[(Q_{20} + 4Q_{00}) \mathcal{L}_{21}^- + 3Q_{20} \mathcal{L}_{11}^- \right] \\
&\quad + \underbrace{2\alpha\kappa_0 \bar{Q}_{20} (3\bar{\mathcal{L}}_{11}^- - \bar{\mathcal{L}}_{21}^-) + \frac{3}{8} \hbar^2 \chi \frac{I_2}{A_1 A_2} \left[(\bar{Q}_{20} + 4\bar{Q}_{00}) \bar{\mathcal{L}}_{21}^- + 3\bar{Q}_{20} \bar{\mathcal{L}}_{11}^- \right] - 6\sqrt{2}\alpha\kappa_0 \bar{L}_{10}^-(\text{eq}) \bar{\mathcal{R}}_{21}^+}_{},
\end{aligned}$$

$$\begin{aligned}
\dot{\mathcal{P}}_{22}^{\uparrow\downarrow} &= -2 [m\omega^2 - 2\kappa_0 Q_{20}] \mathcal{L}_{22}^{\uparrow\downarrow} - i\hbar \frac{\eta}{2} \mathcal{P}_{21}^+ + \frac{3}{2} \hbar^2 \chi \frac{I_2}{A_1 A_2} (Q_{20} + Q_{00}) \mathcal{L}_{22}^{\uparrow\downarrow} \\
&\quad + \underbrace{4\alpha\kappa_0 \bar{Q}_{20} \bar{\mathcal{L}}_{22}^{\uparrow\downarrow} + \frac{3}{2} \hbar^2 \chi \frac{I_2}{A_1 A_2} (\bar{Q}_{20} + \bar{Q}_{00}) \bar{\mathcal{L}}_{22}^{\uparrow\downarrow}}_{}, \\
\dot{\mathcal{P}}_{20}^{\uparrow\downarrow} &= -2 [m\omega^2 + 2\kappa_0 Q_{20}] \mathcal{L}_{20}^{\uparrow\downarrow} + 4\sqrt{2}\kappa_0 Q_{20} \mathcal{L}_{00}^{\uparrow\downarrow} - i\hbar \frac{\eta}{2} \sqrt{\frac{3}{2}} \mathcal{P}_{21}^+ + \frac{3}{2} \hbar^2 \chi \frac{I_2}{A_1 A_2} [Q_{00} \mathcal{L}_{20}^{\uparrow\downarrow} + Q_{20} \mathcal{L}_{00}^{\uparrow\downarrow} / \sqrt{2}] \\
&\quad + \underbrace{4\alpha\kappa_0 \bar{Q}_{20} (\sqrt{2} \bar{\mathcal{L}}_{00}^{\uparrow\downarrow} - \bar{\mathcal{L}}_{20}^{\uparrow\downarrow}) + \frac{3}{2} \hbar^2 \chi \frac{I_2}{A_1 A_2} [\bar{Q}_{00} \mathcal{L}_{20}^{\uparrow\downarrow} + \bar{Q}_{20} \bar{\mathcal{L}}_{00}^{\uparrow\downarrow} / \sqrt{2}]}_{}, \\
\dot{\mathcal{L}}_{00}^{\uparrow\downarrow} &= \frac{1}{m} \mathcal{P}_{00}^{\uparrow\downarrow} - m\omega^2 \mathcal{R}_{00}^{\uparrow\downarrow} + 2\sqrt{2}\kappa_0 Q_{20} \mathcal{R}_{20}^{\uparrow\downarrow} + \frac{\hbar^2}{4 A_1 A_2} \left[\left(\chi + \frac{\bar{\chi}}{3} \right) I_1 - \frac{9}{4} \chi I_2 \right] \left[(2Q_{00} + Q_{20}) \mathcal{R}_{00}^{\uparrow\downarrow} + \sqrt{2} Q_{20} \mathcal{R}_{20}^{\uparrow\downarrow} \right] \\
&\quad + \underbrace{2\sqrt{2}\alpha\kappa_0 \bar{Q}_{20} \bar{\mathcal{R}}_{20}^{\uparrow\downarrow} + \frac{\hbar^2}{4 A_1 A_2} \left[\left(\chi - \frac{\bar{\chi}}{3} \right) I_1 - \frac{9}{4} \chi I_2 \right] \left[(2\bar{Q}_{00} + \bar{Q}_{20}) \bar{\mathcal{R}}_{00}^{\uparrow\downarrow} + \sqrt{2} \bar{Q}_{20} \bar{\mathcal{R}}_{20}^{\uparrow\downarrow} \right]}_{}, \\
\dot{\mathcal{R}}_{00}^{\uparrow\downarrow} &= \frac{2}{m} \mathcal{L}_{00}^{\uparrow\downarrow}, \\
\dot{\mathcal{P}}_{00}^{\uparrow\downarrow} &= -2m\omega^2 \mathcal{L}_{00}^{\uparrow\downarrow} + 4\sqrt{2}\kappa_0 Q_{20} \mathcal{L}_{20}^{\uparrow\downarrow} + \frac{3}{4} \hbar^2 \chi \frac{I_2}{A_1 A_2} \left[(2Q_{00} + Q_{20}) \bar{\mathcal{L}}_{00}^{\uparrow\downarrow} + \sqrt{2} Q_{20} \bar{\mathcal{L}}_{20}^{\uparrow\downarrow} \right] \\
&\quad + \underbrace{4\sqrt{2}\alpha\kappa_0 \bar{Q}_{20} \bar{\mathcal{L}}_{20}^{\uparrow\downarrow} + \frac{3}{4} \hbar^2 \chi \frac{I_2}{A_1 A_2} \left[(2\bar{Q}_{00} + \bar{Q}_{20}) \bar{\mathcal{L}}_{00}^{\uparrow\downarrow} + \sqrt{2} \bar{Q}_{20} \bar{\mathcal{L}}_{20}^{\uparrow\downarrow} \right]}_{}, \\
\dot{\mathcal{P}}_{21} &= -\frac{1}{\hbar} \Delta(r') \mathcal{P}_{21}^+ + \underbrace{6\hbar\kappa_0 K_0 \mathcal{R}_{21}^+ - \frac{1}{\hbar} \bar{\Delta}(r') \bar{\mathcal{P}}_{21}^+ + 6\hbar\alpha\kappa_0 \bar{K}_0 \bar{\mathcal{R}}_{21}^+}_{}, \\
\dot{\mathcal{L}}_{21} &= -\frac{1}{\hbar} \Delta(r') \mathcal{L}_{21}^- - \underbrace{\frac{1}{\hbar} \bar{\Delta}(r') \bar{\mathcal{L}}_{21}^-}_{}, \\
\dot{\mathcal{L}}_{11} &= -\frac{1}{\hbar} \Delta(r') \mathcal{L}_{11}^- - \underbrace{\frac{1}{\hbar} \bar{\Delta}(r') \bar{\mathcal{L}}_{11}^-}_{}, \tag{23}
\end{aligned}$$

where the terms coupling isovector and isoscalar sets of equations are underlined by the braces and

$$\begin{aligned}
A_1 &= \sqrt{2} R_{20}^{\text{eq}} - R_{00}^{\text{eq}} = \frac{Q_{00}}{\sqrt{3}} \left(1 + \frac{4}{3} \delta \right), \\
A_2 &= R_{20}^{\text{eq}} / \sqrt{2} + R_{00}^{\text{eq}} = -\frac{Q_{00}}{\sqrt{3}} \left(1 - \frac{2}{3} \delta \right), \tag{24}
\end{aligned}$$

$Q_{00} = \frac{3}{5} A R^2 / [(1 + \frac{4}{3} \delta)^{1/3} (1 - \frac{2}{3} \delta)^{2/3}]$,
 δ - deformation parameter, $Q_{20} = \frac{4}{3} \delta Q_{00}$,
 $\bar{Q}_{00} = Q_{00}^{\text{n}} - Q_{00}^{\text{p}}$, $\bar{Q}_{20} = Q_{20}^{\text{n}} - Q_{20}^{\text{p}}$,
 $\bar{\Delta} = \Delta^{\text{n}} - \Delta^{\text{p}}$, $R = r_0 A^{1/3}$, $r_0 = 1.2$ fm,

$$I_1 = \frac{\pi}{4} \int_0^\infty dr r^4 \left(\frac{\partial n(r)}{\partial r} \right)^2, \quad I_2 = \frac{\pi}{4} \int_0^\infty dr r^2 n(r)^2,$$

$n(r) = n_0 \left(1 + e^{\frac{r-R}{a}} \right)^{-1}$ - nuclear density, $a = 0.53$,

$$K_0 = \int d(\mathbf{r}, \mathbf{p}) \kappa_0(\mathbf{r}, \mathbf{p}), \quad \bar{K}_0 = K_0^{\text{n}} - K_0^{\text{p}}.$$

The functions $\Delta(r')$, $I_{pp}^{\kappa\Delta}(r')$ and $I_{pp}^{\Delta}(r')$ are outlined in Appendix. Deriving these equations we neglected double Poisson brackets containing κ or Δ ,

which are the quantum corrections to pair correlations.

V. RESULTS OF CALCULATIONS AND DISCUSSION

The calculations were performed for nuclei of the $N = 82 - 126$ mass region and for Actinides. The calculations procedure and parameters are mostly the same as in our previous paper [13].

A. Nuclei of the $N = 82 - 126$ mass region

1. WFM

Let us analyze in detail the results of systematic calculations for nuclei of this mass region considering the example of Dy isotopes. The most interesting of them is ^{164}Dy , where a rather exceptional experimental situation with the low-lying 1^+ excitations exists. The results of the solution of equations (22, 23) for this nucleus are presented in the

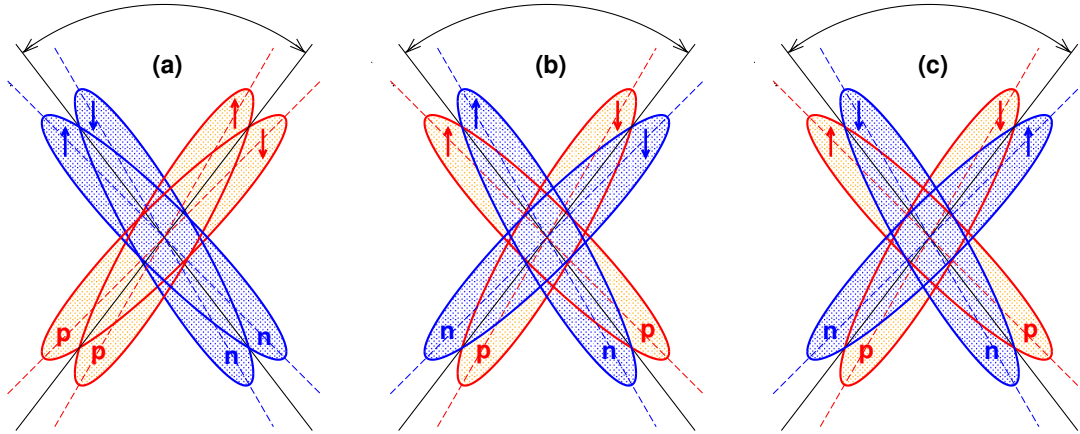


FIG. 2: Schematic representation of three scissors modes: (a) spin-scalar isovector (conventional, orbital scissors), (b) spin-vector isoscalar (spin scissors), (c) spin-vector isovector (spin scissors). Arrows show the direction of spin projections; p – protons, n – neutrons. The small angle spread between the various distributions is only for presentation purposes. In reality the distributions are perfectly overlapping.

Table I, where the energies of 1^+ levels with their magnetic dipole and electric quadrupole strengths are shown. Left panel – the solutions of decoupled equations, right – isoscalar-isovector coupling is taken into account. The first observation is that

TABLE I: The results of WFM calculations for ^{164}Dy for energies E (MeV), magnetic dipole $B(M1)$ (μ_N^2) and electric quadrupole $B(E2)$ (W. u.) strengths of 1^+ excitations. The marks IS – isoscalar and IV – isovector are valid only for the decoupled case.

	Decoupled equations			Coupled equations		
	E	$B(M1)$	$B(E2)$	E	$B(M1)$	$B(E2)$
IS	1.29	0.01	53.25	1.47	0.17	25.44
IV	2.44	2.03	0.34	2.20	1.76	3.30
IS	2.62	0.09	2.91	2.87	2.24	0.34
IV	3.35	1.36	1.62	3.59	1.56	4.37
IS	10.94	0.00	55.12	10.92	0.04	50.37
IV	14.04	0.00	2.78	13.10	0.00	2.85
IS	14.60	0.06	0.48	15.42	0.07	0.57
IV	15.88	0.00	0.55	15.55	0.00	1.12
IS	16.46	0.07	0.36	16.78	0.06	0.53
IV	17.69	0.00	0.45	17.69	0.01	0.68
IS	17.90	0.00	0.51	17.91	0.00	0.53
IV	18.22	0.18	1.85	18.22	0.13	0.89
IS	19.32	0.10	0.97	19.32	0.08	0.61
IV	21.29	2.47	31.38	21.26	2.03	21.60

the high-lying levels are less sensitive to decoupling. Among the high-lying states, $\mu = 1$ branches of isoscalar (at the energy of 10.92 MeV) and isovector ($E = 21.26$ MeV) Giant Quadrupole Resonances are distinguished by the large $B(E2)$ values. The rest of high-lying states have quite small excitation proba-

bilities and we omit them from further discussion.

Comparing the left and right panels, we see that the most remarkable change happens with the third low-lying level, an isoscalar one without coupling, – it acquires a rather big magnetic strength. The ”jump” from $0.09 \mu_N^2$ to $2.24 \mu_N^2$ looks a little bit surprising. However it is explained quite naturally by the structure of the matrix element of the excitation operator (see Appendix C). According to formula (C6) the contribution of isoscalar variables occurs with the factor $[g_s^n + g_s^p - g_t^p]$. Its numerical value (including the quenching factor $q = 0.7$) is 0.23. The contribution of isovector variables goes with the factors $\frac{1}{2}(g_s^p - g_s^n) = 3.29$ and $g_t^p = 1$, i.e. ~ 20 times bigger than isoscalar one. In the decoupled case the third level, being the isoscalar one, has the contribution only from isoscalar variables, which is obviously small. In the case with coupling it gets the additional contribution from isovector variables, which is an order of magnitude bigger. This explains the effect of the big increase of the $B(M1)$ value.

So, in the decoupled case there are 2 isoscalar electric and 2 isovector magnetic low-lying levels, and in the coupled case there are 1 electric and 3 magnetic levels of mixed isovector-isoscalar nature. The interpretation of the lowest electric level is not clear at this moment and requires the separate investigation. It shows practically zero $B(M1)$ strength and, thus, is not of direct interest to this work. Its nature shall be studied in future work.

The three magnetic states correspond to three physically possible types of scissors modes already mentioned in the introduction. Roughly speaking the state at the energy 3.59 MeV in ^{164}Dy is predominately the conventional ”orbital” scissors mode, the last two states at the energies 2.20 MeV and 2.87 MeV are predominately the ”spin” scissors modes.

The detailed analysis of these three states is given in section C, "Currents".

The Fig. 2 shows a schematic representation of these modes: the orbital scissors (neutrons versus protons) and two spin scissors (spin-up nucleons versus spin-down nucleons and more complicated – spin-up protons together with spin-down neutrons versus spin-down protons with spin-up neutrons). Both spin scissors exist only due to spin degrees of freedom. If we remove the arrows from the picture, nothing will change for the conventional scissors (a). However figures (b) and (c) in this case become identical and senseless, because the division of identical particles (neutrons or protons) in two parts becomes irrelevant.

The natural question arises here: what is the origin of forces who coerce the spin-up and spin-down particles to move out of phase? There is no analogous problem with the conventional scissors, because the Hamiltonian (6) includes the neutron-proton quadrupole-quadrupole (q-q) interaction (7), that makes protons and neutrons move out of phase. But what generates a similar motion of spin-up and spin-down particles? It turns out that again the main working element is the nucleon-nucleon q-q interaction. However, this time it works together with the spin-orbital part of the mean field.

Let us consider in detail the "life" of, for example, the system of spin-up protons and spin-down neutrons within the mean field. Due to the neutron-proton q-q interaction protons push neutrons and force them to move generating in such a way for example the scissors modes (Fig. 2b)). Neutrons have spins, so due to the spin-orbital term their motion will depend on their spin projection. That means that the result of pushing will depend on the spin projections of the pushed neutrons. In addition, the pushing protons also have spins, therefore the result of pushing will depend on their spin projection too. Moreover, due to proton-proton q-q interaction spin-up protons will push spin-down protons and again the result of their interaction will be influenced by the spin-orbital potential. As we see, there is no necessity to introduce the special kind of interaction to activate the spin degrees of freedom and to generate in such a way the spin dependent excitation. It is done quite naturally by the usual q-q interaction, the result of the activation being dependent on spin projections due to the spin-orbital potential, which can lead to the appearance of three different types of scissors.

So, the calculations without an artificial decoupling produce three low-lying magnetic states (instead of two without coupling). The energies and $B(M1)$ values of all three types of scissors calculated for other nuclei are shown in Tables II, III.

In our example of ^{164}Dy the summarized magnetic strength $\sum B(M1) = 5.56 \mu_N^2$ of three scis-

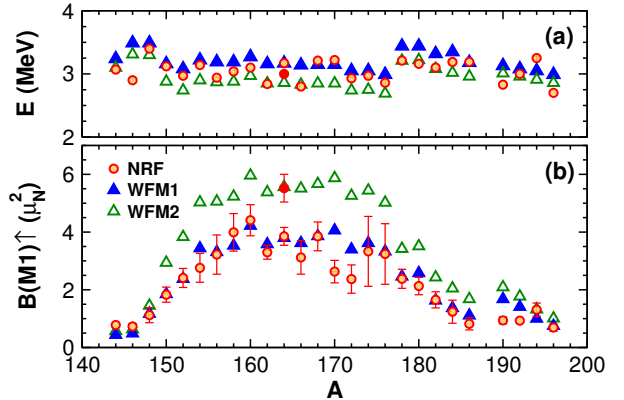


FIG. 3: Calculated (WFM) and experimental (NRF) mean excitation energies (a) and summed $M1$ strengths (b) of the scissors mode. WFM1 – the sum of two highest scissors, WFM2 – the sum of three scissors. Experimental data are taken from the papers listed in the Table 1 of [15]. The solid circle marks the experimental result for ^{164}Dy when summed in the energy range from 2 to 4 MeV.

sors is remarkably stronger than the analogous value $\sum B(M1) = 3.39 \mu_N^2$ of two magnetic states in the case of decoupling (see Table I). One may say that it is also stronger than the respective experimental value. However, one must be careful here.

Trying to compare the theoretical results with the existing experimental data for the scissors mode, we encounter different summing interval conventions. It is assumed that the scissors mode includes only the states in a certain energy range. As a rule, the following two conventions are chosen, which lead to slightly different results for the summed $M1$ strength:

- 2.7 < E < 3.7 MeV for $Z < 68$ and
- 2.4 < E < 3.7 MeV for $Z \geq 68$ [14],
- 2.5 < E < 4.0 MeV for $82 \leq N \leq 126$ [15].

Obviously, only the two highest scissors fall into both of these intervals. It turns out that their summed $B(M1)$ agrees rather well with the majority of experimental values found by NRF (Nuclear Resonance Fluorescence) experiments [14–16] for nuclei of $N = 82 - 126$ mass region (see Fig. 3 and columns 6 and 13 of Table VI). The situation with the lowest scissors is very interesting. It helps to explain the long-standing problem of the 1^+ spectrum of ^{164}Dy .

The Fig. 4 demonstrates experimental $M1$ strength distributions in $^{160,162,164}\text{Dy}$ in the energy range between 2 MeV and 4 MeV, reported by Margraf *et al.* [17]. Obviously, there are two groups of strong $M1$ excitations in ^{164}Dy around 2.6 and 3.1 MeV. However, only the upper group was attributed to the scissors mode, and the group around 2.6 MeV was not included because it has a rather big spin contribution and one level has pure two-

TABLE II: The nuclear scissors mode fine structure. The results of calculations by the WFM method: energies E_i with correspondings $B_i(M1)$ -values. Energy centroids \bar{E} and summed $M1$ strength are also presented. Parameters of pair correlations: $V_0^p = 27$ MeV, $V_0^n = 23$ MeV, $r_p^p = 1.50$ fm, $r_p^n = 1.85$ fm for nuclei with $A = 150 - 186$. The spin-orbit strength constant $\kappa_{\text{NiIs}} = 0.0637$, quenching factor $q = 0.7$. Parameters that differ from those indicated: $V_0^p = 26.5$ MeV, $V_0^n = 22.6$ MeV for Hf and W isotops, $q = 0.57$ for ^{150}Sm , $r_p^p = 1.57$ fm, $q = 0.78$ for ^{150}Nd , $V_0^p = 23$ MeV, $V_0^n = 20$ MeV, $r_p^p = 2.0$ fm, $r_p^n = 2.4$ fm, $q = 0.5$ for ^{148}Sm and ^{148}Nd , $V_0^p = 23$ MeV, $V_0^n = 20$ MeV, $r_p^p = 2.05$ fm, $r_p^n = 2.5$ fm, $\kappa_{\text{NiIs}} = 0.05$, $q = 0.5$ for ^{146}Nd .

Nuclei	δ	i	E_i (MeV)	$B_i(M1)$ (μ_N^2)		$\bar{E}_{[2-3]}$ (MeV)		$\sum_{i=2}^3 B_i(M1)$ (μ_N^2)		$\bar{E}_{[1-3]}$ (MeV)	$\sum_{i=1}^3 B_i(M1)$ (μ_N^2)
				WFM		WFM	NRF	WFM	NRF		
^{146}Nd	0.13	1	2.66	0.13							
		2	3.41	0.38	3.49	2.90	0.49	0.73(10)	3.31	0.63	
		3	3.74	0.12							
^{148}Nd	0.17	1	2.51	0.28							
		2	3.36	0.80	3.49	3.40	1.17	1.12(26)	3.30	1.45	
		3	3.78	0.37							
^{150}Nd	0.23	1	2.39	1.08							
		2	3.07	1.57	3.16	3.12	1.85	1.83(27)	2.88	2.94	
		3	3.70	0.28							
^{148}Sm	0.12	1	2.48	0.08							
		2	3.16	0.19	3.21	3.07	0.23	0.51(12)	3.02	0.31	
		3	3.48	0.04							
^{150}Sm	0.16	1	2.27	0.49							
		2	2.68	0.23	3.00	3.18	0.61	0.97(17)	2.67	1.10	
		3	3.18	0.38							
^{152}Sm	0.24	1	2.18	1.45							
		2	2.75	1.31	3.08	2.97	2.38	2.41(33)	2.74	3.83	
		3	3.48	1.07							
^{154}Sm	0.26	1	2.22	1.59							
		2	2.91	1.98	3.22	3.14	3.44	2.76(50)	2.90	5.03	
		3	3.64	1.46							
^{154}Gd	0.25	1	2.24	1.70							
		2	2.78	1.40	3.12	3.00	2.65	2.60(5)	2.78	4.35	
		3	3.51	1.25							
^{156}Gd	0.26	1	2.25	1.75							
		2	2.86	1.84	3.19	2.94	3.31	3.22(68)	2.87	5.06	
		3	3.60	1.46							
^{158}Gd	0.26	1	2.22	1.70							
		2	2.88	2.04	3.19	3.04	3.53	3.99(65)	2.88	5.23	
		3	3.61	1.49							
^{160}Gd	0.27	1	2.23	1.74							
		2	2.97	2.50	3.27	3.10	4.22	4.41(54)	2.97	5.96	
		3	3.70	1.72							
^{160}Dy	0.26	1	2.25	1.84							
		2	2.84	1.85	3.17	2.87	3.35	2.42(30)	2.84	5.19	
		3	3.56	1.50							
^{162}Dy	0.26	1	2.22	1.80							
		2	2.86	2.04	3.16	2.84	3.58	3.30(24)	2.85	5.38	
		3	3.57	1.53							
^{164}Dy	0.26	1	2.20	1.76							
		2	2.87	2.24	3.17	3.17	3.80	3.85(31)	2.86	5.56	
		3	3.59	1.56							

TABLE III: Continuation of Table II.

Nuclei	δ	i	E_i (MeV)	$B_i(M1)$ (μ_N^2)		$\bar{E}_{[2-3]}$ (MeV)		$\sum_{i=2}^3 B_i(M1)$ (μ_N^2)		$\bar{E}_{[1-3]}$ (MeV)	$\sum_{i=1}^3 B_i(M1)$ (μ_N^2)
				WFM		WFM	NRF	WFM	NRF		
^{166}Er	0.26	1	2.23		1.89						
		2	2.83		2.05	3.14	2.79	3.62	3.12(58)	2.83	5.51
		3	3.54		1.57						
^{168}Er	0.26	1	2.20		1.81						
		2	2.87		2.28	3.15	3.21	3.86	3.85(50)	2.85	5.67
		3	3.57		1.58						
^{170}Er	0.26	1	2.18		1.81						
		2	2.86		2.43	3.15	3.22	4.06	2.63(39)	2.85	5.87
		3	3.57		1.63						
^{172}Yb	0.25	1	2.18		1.86						
		2	2.76		1.97	3.05	2.93	3.40	2.37(49)	2.74	5.26
		3	3.45		1.43						
^{174}Yb	0.25	1	2.16		1.82						
		2	2.78		2.16	3.05	2.96	3.62	3.33(1.21)	2.75	5.44
		3	3.46		1.46						
^{176}Yb	0.24	1	2.11		1.69						
		2	2.73		2.04	2.99	2.86	3.33	3.24(1.05)	2.69	5.02
		3	3.40		1.29						
^{176}Hf	0.23	1	2.66		1.08						
		2	3.36		1.96	3.50	3.22	2.71	3.32(28)	3.26	3.79
		3	3.86		0.76						
^{178}Hf	0.22	1	2.62		0.96						
		2	3.33		1.89	3.44	3.21	2.46	2.38(33)	3.21	3.42
		3	3.82		0.58						
^{180}Hf	0.22	1	2.60		0.93						
		2	3.34		2.04	3.44	3.16	2.58	2.13(30)	3.22	3.51
		3	3.83		0.54						
^{182}W	0.20	1	2.59		0.80						
		2	3.23		1.30	3.32	3.10	1.63	1.65(28)	3.08	2.43
		3	3.68		0.33						
^{184}W	0.19	1	2.56		0.68						
		2	3.20		1.20	3.35	3.19	1.37	1.24(37)	3.02	2.05
		3	3.63		0.17						
^{186}W	0.18	1	2.53		0.57						
		2	3.17		1.09	3.18	3.19	1.11	0.82(21)	2.96	1.68
		3	3.59		0.02						

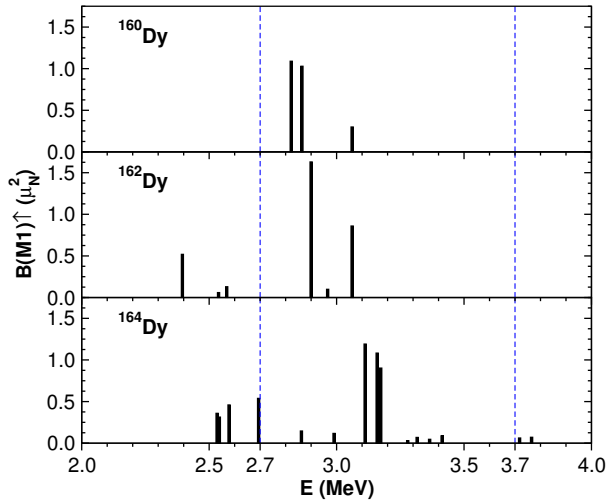


FIG. 4: Excitation energies E with the corresponding $B(M1)$ values, obtained by the NRF experiment [17]. The dashed lines mark the boundaries of the conventional interval from [14].

quasiparticle nature and the summed $M1$ strength of both groups strongly deviates from the scissors mode systematics in the Rare Earth nuclei [15]. The results of our calculations allow one to clarify the origin of both groups. Table IV demonstrates that the energy centroid and summed $B(M1)$ -value of the observed lower group agree very well with the calculated energy E and $B(M1)$ value of the lowest scissors. The respective values of the observed higher group are in excellent agreement with the calculated energy centroid and summed $B(M1)$ of two remaining (higher in energy) scissors.

TABLE IV: The calculated energies E (MeV) and excitation probabilities $B(M1)$ (μ_N^2) of three scissors are compared with experimental values \bar{E} and $\sum B(M1)$ of two groups of 1^+ levels in ^{164}Dy [17].

Theory (WFM)				Experiment (NRF)	
E	$B(M1)$	\bar{E}	$\sum B(M1)$	\bar{E}	$\sum B(M1)$
2.20	1.76	2.20	1.76	2.60	1.67(14)
2.87	2.24	3.17	3.80	3.17	3.85(31)
3.59	1.56				

So, according to our calculations, the low-energy group of states in ^{164}Dy is also a branch of the scissors mode (spin-vector isovector scissors) and the calculated summed magnetic strength $5.56 \mu_N^2$ is in excellent agreement with the experimental value $5.52 \mu_N^2$. Analogous values for two other Dy isotopes, ^{160}Dy and ^{162}Dy , are predicted to be $5.19 \mu_N^2$ and $5.38 \mu_N^2$ (see Table V). From a first glance on Fig. 4 it becomes clear that in those nuclei nothing similar to the ^{164}Dy case was observed by

NRF experiments. Nevertheless our prediction was confirmed recently by another experiment – photo-neutron measurements performed by the Oslo group. In Ref. [18] the authors revised their previous data on the Scissors Resonance (SR) in $^{160-164}\text{Dy}$ obtained by the Oslo method. The essence of their findings is formulated in the following quotation from [18]: “...If we integrate Eq. (19) over all transition energies, we find a total, summed SR strength of $4.6(12) - 5.8(26)\mu_N^2$... The present fit strategy gives about 40% higher summed SR strengths than the reported NRF results. However, if we apply the NRF energy limits to Eq. (19), we obtain excellent agreement with the NRF results... It is interesting to note that $\approx 40 - 60\%$ of our measured SR strength lies in the energy region below 2.7 MeV. In traditional NRF experiments using bremsstrahlung, the transitions in this energy range are quite difficult to separate from the sizable atomic background.”

This is exactly the point! The statements about “40% higher” and “ $\approx 40 - 60\%$... below 2.7 MeV” are in qualitative and often in very good agreement with our findings!

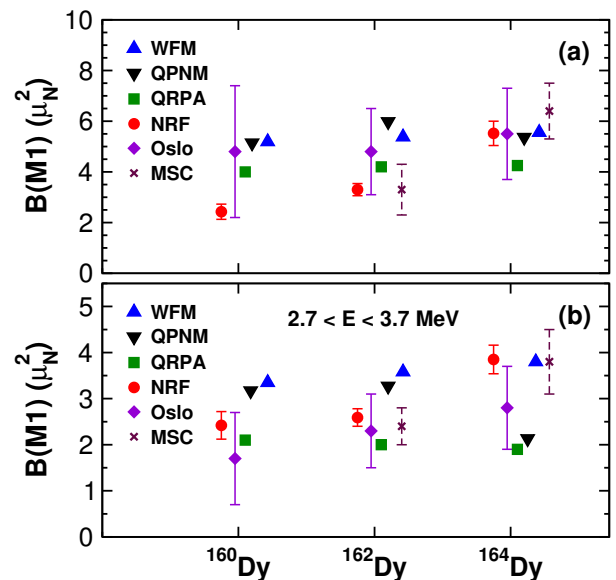


FIG. 5: Comparison of the summed $B(M1)$ values for SR in $^{160,162,164}\text{Dy}$ from the present WFM theory, the QPNM [19, 20] and Gogny QRPA [18] calculations with the experimental values from the NRF [17], photo-neutron measurements (Oslo) [18] and from multistep-cascade (MSC) measurements of γ decay following neutron capture [21]. Panel (a) – averaging energy intervals are 2 – 4 MeV for WFM, QPNM and NRF; 0 – 3.5 MeV for QRPA; 0 – 10 MeV for Oslo and MSC, (b) – averaging interval is 2.7 – 3.7 MeV.

TABLE V: The energy centroids \bar{E} and corresponding summed $B(M1)$ values given by WFM theory and QPNM calculations are compared with experimental results by the NRF [17] and photo-neutron measurements (Oslo) [18] for $^{160,162,164}\text{Dy}$. Comparison is presented for various energy intervals.

^ADy	Theory				Experiment			
	WFM		QPNM		NRF		Oslo	
	\bar{E} (MeV)	$B(M1)$ (μ_N^2)	\bar{E} (MeV)	$B(M1)$ (μ_N^2)	\bar{E} (MeV)	$B(M1)$ (μ_N^2)	\bar{E} (MeV)	$B(M1)$ (μ_N^2)
	$2.7 < E < 3.7$ MeV				$2.7 < E < 3.7$ MeV			
^{160}Dy	3.17	3.35	3.05	3.17	2.87	2.42(30)	2.66(12)	1.7(10)
^{162}Dy	3.16	3.58	3.08	3.27	2.96	2.59(19)	2.81(8)	2.3(8)
^{164}Dy	3.17	3.80	3.26	2.13	3.17	3.85(31)	2.83(8)	2.8(9)
	$2.0 < E < 4.0$ MeV				$2.0 < E < 4.0$ MeV		$0 < E < 10$ MeV	
^{160}Dy	2.84	5.19	3.05	5.14	2.87	2.42(30)	2.66(12)	4.8(26)
^{162}Dy	2.85	5.38	3.10	5.98	2.84	3.30(24)	2.81(8)	4.8(17)
^{164}Dy	2.86	5.56	2.87	5.36	3.00	5.52(48)	2.83(8)	5.5(18)

2. WFM versus QPNM

In the rest nuclei of $N = 82 - 126$ mass region an equally significant low energy $M1$ strength was not detected in the NRF experiments. However, our calculations predict the existence of comparable magnetic strength in all well-deformed nuclei of this mass region (see WFM2 in Fig. 3). This prediction is supported by calculations in the frame of Quasiparticle-Phonon Nuclear Model (QPNM), which also predicts remarkable $M1$ strength below the conventional energy interval. A short outline of QPNM together with calculation details can be found in the papers [19, 20].

The energy centroids and corresponding summed $B(M1)$ given by the WFM theory and by the QPNM calculations for Dy isotopes are compared with experimental results from the NRF and from photo-neutron measurements (Oslo) [18] in Table V. The

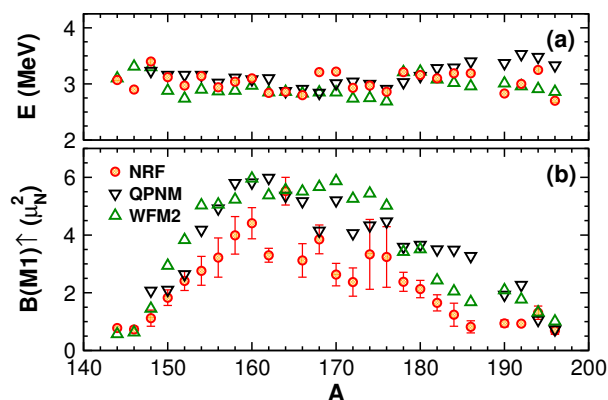


FIG. 6: WFM2 – energy centroid of three scissors and the respective $B(M1)$ value given by WFM method, QPNM – analogous values calculated in the frame of QPNM in the energy range 2 – 4 MeV, NRF – experimental data.

results are shown for various energy averaging intervals. As it is seen, the theoretical results and experimental data of Oslo group are in very good overall agreement for all three Dy isotopes. It is worthwhile to remark the excellent agreement between all theoretical and experimental results for ^{164}Dy . One may be worried by the comparatively big interval $0 < E < 10$ MeV employed by the Oslo group [18] for centroids energies and $B(M1)$. However, in their paper they say that all spin-flip excitations are eliminated in their averages and, thus, their averaging becomes equal to the theoretical one, since it is generally believed that all what is above 4 MeV excitation energy does not belong to SR excitations. In Fig. 5 the summed $B(M1)$ values are also shown for $^{160,162,164}\text{Dy}$ including this time the results from Gogny QRPA calculations and the experimental results obtained by the radiative capture of resonance neutrons [21]. It is remarkable to which extent theory and experiment agree taking the NRF as well as the Oslo averaging intervals. This yields strong support to our interpretation that there are in fact not one but three intermingled scissors modes at play: the conventional one and two spin scissors which may be predominately isovector spin-vector and isoscalar spin-vector in nature. As mentioned, this is just the natural triplet of scissors modes which one obtains from pure combinatorics.

The energy centroids and summed $B(M1)$ values of two highest scissors are compared with the experimental NRF data in the columns 6, 7 and 8, 9 of Tables II, III. This comparison is demonstrated also in Fig. 3. It is seen that the overall agreement between the theoretical and experimental results is very good – there are only 3 (of 27) remarkable differences for $B(M1)$ (^{160}Dy , ^{170}Er , ^{172}Yb) and four ones for energies (^{146}Nd , $^{160,162}\text{Dy}$, ^{166}Er). The energy centroids and summed $B(M1)$ values of all three scissors are shown in columns 10 and 11. These data are

TABLE VI: The analysis of the nuclear scissors mode structure for specific energy regions. The results of calculations by the WFM method and QPNM: energies E_i with correspondings $B_i(M1)$. The energy ranges for QPNM are: I: 1.8 – 4.0 MeV ($i = 1$: 1.8 – 2.5 MeV, $i = 2$: 2.5 – 4.0 MeV); II: 1.8 – 3.7 MeV ($i = 1$: 1.8 – 2.7 MeV, $i = 2$: 2.7 – 3.7 MeV). Energy centroids \bar{E} and summed $M1$ strength from WFM, QPNM calculations and NRF experiments are presented for specified energy ranges. The parameter values for WFM calculations are indicated in the caption to Table II.

Nuclei	i	E_i (MeV)		$B_i(M1)$ (μ_N^2)			NRF	\bar{E} (MeV)			$\sum B(M1)$ (μ_N^2)				
		WFM	QPNM	WFM	QPNM	QPNM		WFM	QPNM	NRF	WFM	QPNM	QPNM		
			I	II	I	II		I	II	2.0 – 4.0	1.8 – 4.0	1.8 – 4.2	2.0 – 4.0	1.8 – 4.0	1.8 – 4.2
^{148}Nd	1	2.51	2.47	2.47	0.28	0.41	0.41	3.40	3.30	3.23	3.25	1.12(26)	1.45	2.07	2.11
	2	3.49	3.42	3.18	1.17	1.65	1.15								
^{150}Nd	1	2.39	2.46	2.46	1.08	0.52	0.52	3.12	2.88	3.16	3.17	1.83(27)	2.94	2.10	2.13
	2	3.16	3.39	3.18	1.85	1.59	1.13								
^{148}Sm	1	2.48	2.43	2.55	0.08	0.22	0.74	3.07	3.02	2.88	3.25	0.51(12)	0.31	1.57	2.24
	2	3.21	2.95	3.17	0.23	1.36	0.83								
^{150}Sm	1	2.27	–	2.53	0.49	–	0.40	3.18	2.67	3.11	3.38	0.97(17)	1.10	1.59	2.17
	2	3.00	3.11	3.30	0.61	1.59	1.17								
^{152}Sm	1	2.18	2.31	2.31	1.45	0.13	0.13	2.97	2.74	3.16	3.40	2.41(33)	3.83	2.64	3.50
	2	3.08	3.21	3.21	2.38	2.51	2.50								
^{154}Sm	1	2.22	2.19	2.19	1.59	0.83	0.83	3.14	2.90	3.16	3.22	2.76(50)	5.03	4.18	4.45
	2	3.22	3.41	3.28	3.44	3.34	2.67								
^{156}Gd	1	2.25	2.04	2.04	1.75	0.79	0.79	2.94	2.87	3.02	3.10	3.22(68)	5.06	4.92	5.30
	2	3.19	3.20	3.15	3.31	4.13	3.81								
^{158}Gd	1	2.22	2.34	2.34	1.70	0.48	0.48	3.04	2.88	3.11	3.13	3.99(65)	5.23	5.80	5.87
	2	3.19	3.18	3.08	3.53	5.32	4.64								
^{160}Gd	1	2.23	2.47	2.56	1.74	0.63	1.28	3.10	2.97	3.08	3.13	4.41(54)	5.96	5.82	6.14
	2	3.27	3.15	3.10	4.22	5.18	3.79								
^{160}Dy	1	2.25	2.43	2.43	1.84	1.07	1.08	2.87	2.84	3.05	3.14	2.42(30)	5.19	5.14	5.62
	2	3.17	3.22	3.05	3.35	4.07	3.17								
^{162}Dy	1	2.22	2.46	2.47	1.80	1.40	1.41	2.84	2.85	3.10	3.11	3.30(24)	5.38	5.98	6.05
	2	3.16	3.30	3.08	3.58	4.58	3.27								
^{164}Dy	1	2.20	2.08	2.35	1.76	1.26	2.69	3.00	2.86	2.87	2.89	5.52(48)	5.56	5.36	5.45
	2	3.17	3.11	3.26	3.80	4.10	2.13								
^{166}Er	1	2.23	2.04	2.29	1.89	1.35	2.30	2.79	2.83	2.91	2.95	3.12(58)	5.51	5.17	5.36
	2	3.14	3.21	3.24	3.62	3.82	2.13								
^{168}Er	1	2.20	2.32	2.48	1.81	1.14	2.20	3.21	2.85	2.84	2.85	3.85(50)	5.67	4.15	4.21
	2	3.15	3.03	3.19	3.86	3.01	1.81								
^{172}Yb	1	2.18	2.16	2.52	1.86	0.53	1.96	2.93	2.74	3.04	3.07	2.37(49)	5.26	4.06	4.19
	2	3.05	3.17	3.27	3.40	3.53	1.22								
^{174}Yb	1	2.16	2.10	2.40	1.82	0.86	1.89	2.96	2.75	3.00	3.00	3.33(1.21)	5.44	4.33	4.34
	2	3.05	3.22	3.33	3.62	3.48	1.83								
^{176}Yb	1	2.11	1.88	2.26	1.69	1.11	2.20	2.86	2.69	2.91	2.91	3.24(1.05)	5.02	4.47	4.47
	2	2.99	3.25	3.54	3.33	3.36	2.27								
^{176}Hf	1	2.66	2.21	2.21	1.08	1.04	1.04	3.22	3.26	3.12	3.12	3.32(28)	3.79	3.93	3.93
	2	3.50	3.45	3.39	2.71	2.89	2.57								
^{178}Hf	1	2.62	2.22	2.27	0.96	0.92	1.04	3.21	3.21	3.03	3.03	2.38(33)	3.42	3.59	3.59
	2	3.44	3.31	3.34	2.46	2.66	2.54								
^{180}Hf	1	2.60	2.29	2.29	0.93	0.79	0.79	3.16	3.22	3.14	3.14	2.13(30)	3.51	3.66	3.66
	2	3.44	3.37	3.18	2.58	2.86	2.01								
^{182}W	1	2.59	2.29	2.52	0.80	0.01	0.13	3.10	3.08	3.28	3.28	1.65(28)	2.43	3.50	3.51
	2	3.32	3.28	3.19	1.63	3.49	2.78								
^{184}W	1	2.56	2.39	2.39	0.68	0.54	0.54	3.19	3.02	3.29	3.29	1.24(37)	2.05	3.49	3.49
	2	3.35	3.45	3.32	1.37	2.96	2.30								
^{186}W	1	2.53	2.40	2.61	0.57	0.01	0.68	3.19	2.96	3.40	3.40	0.82(21)	1.68	3.27	3.28
	2	3.18	3.40	3.50	1.11	3.25	1.98								

TABLE VII: The continuation of Table VI. Parameters for WFM calculations: $V_0^p = 26.5$ MeV, $V_0^n = 22.6$ MeV, $r_p^p = 1.7$ fm, $r_p^n = 2.1$ fm, $\kappa_{\text{NiIs}} = 0.05$, $q = 0.57$.

Nuclei	E_i (MeV)		$B_i(M1)$ (μ_N^2)				\bar{E} (MeV)			$\sum B(M1)$ (μ_N^2)							
	i	WFM QPNM		WFM QPNM		NRF	WFM	QPNM		NRF	QPNM						
		I	II	I	II			2.0 – 4.0	1.8 – 4.0		1.8 – 4.2	2.0 – 4.0	1.8 – 4.0	1.8 – 4.2			
^{190}Os	1	2.51	–	–	0.42	–	–	–	–	2.83	3.01	3.37	3.54	0.94(12)	2.09	1.93	2.55
	2	3.13	3.37	3.36	1.68	1.93	1.91	–	–	–	–	–	–	–	–	–	–
^{192}Os	1	2.49	–	–	0.35	–	–	–	–	3.00	2.96	3.53	3.61	0.93(06)	1.77	2.27	2.65
	2	3.08	3.53	3.44	1.41	2.27	1.73	–	–	–	–	–	–	–	–	–	–
^{194}Pt	1	2.50	2.23	2.38	0.32	0.06	0.11	–	–	3.25	2.91	3.48	3.51	1.31(23)	1.32	1.06	1.11
	2	3.05	3.56	3.34	1.00	1.00	0.48	–	–	–	–	–	–	–	–	–	–
^{196}Pt	1	2.47	2.27	2.35	0.26	0.02	0.03	–	–	2.70	2.86	3.33	3.59	0.69(13)	1.01	0.73	1.14
	2	2.99	3.36	3.24	0.75	0.71	0.55	–	–	–	–	–	–	–	–	–	–

also shown on Fig. 3. Only for ^{164}Dy there is the excellent agreement of the theory and experiment. For all the rest nuclei the significant additional $M1$ strength, given by the WFM method, is a prediction. This prediction is supported by QPNM calculations (see Tables VI, VII and Fig. 6).

B. Actinides

The case of Actinides is similar to the Rare Earth region, see Table VIII and Figs. 7, 8. The calculated energy centroids and summed $B(M1)$ values of two highest scissors in ^{232}Th are in excellent agreement with experimental NRF data. The agreement between the analogous values in ^{236}U can be characterized as acceptable. In addition, Fig. 8 demon-

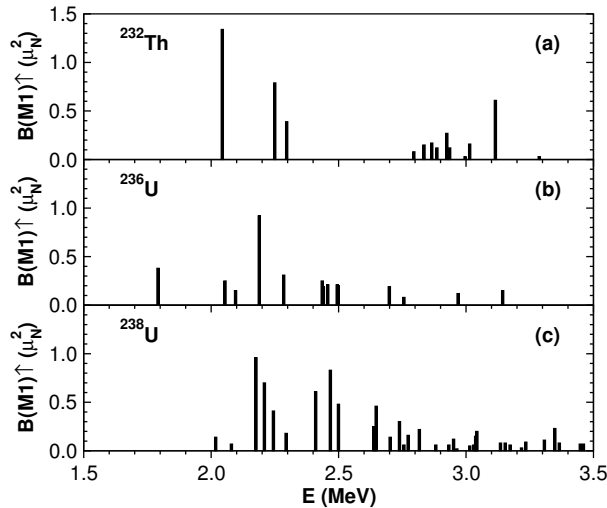


FIG. 7: The experimentally observed spectra of 1^+ excitations in (a) ^{232}Th – [22], (b) ^{236}U – [23] and (c) ^{238}U – [24].

strates that the average energy and the summed magnetic strength of the lower group of levels in ^{232}Th practically exactly coincides with the energy and $B(M1)$ value of the middle ($E = 2.2$ MeV) calculated scissors mode and the analogous values of the higher group of levels are in very good agreement with the energy and $B(M1)$ value of the highest ($E = 2.81$ MeV) scissors mode given by the theory. A similar picture can be obtained for ^{236}U if to divide its spectrum in two groups, the boundary between them being chosen in the energy window $2.3 \text{ MeV} < E < 2.4 \text{ MeV}$ (see Fig. 7). It is worth to note an interesting detail of ^{236}U spectrum. Its lowest level is disposed remarkably lower 2 MeV and is separated by the remarkable energy gap from the higher levels. This makes it possible to interpret this level as a small fraction of the lowest scissors predicted by the theory.

One observes an unexpectedly large value of the summed $B(M1)$ for ^{238}U in comparison with that of ^{236}U and ^{232}Th and with the theoretical result. The possible reason of this discrepancy was indicated by the authors of [24]: “*M1 excitations are observed at approximately $2.0 \text{ MeV} < E_\gamma < 3.5 \text{ MeV}$ with a strong concentration of $M1$ states around 2.5 MeV. ... The observed $M1$ strength may include states from both the scissors mode and the spin-flip mode, which are indistinguishable from each other based exclusively on the use of the NRF technique.*” The most reasonable (and quite natural) place for the boundary between the scissors mode and the spin-flip resonance is located in the spectrum gap between 2.5 MeV and 2.62 MeV (see Fig. 7). The summed $M1$ strength of scissors in this case becomes $B(M1) = 4.38 \pm 0.5 \mu_N^2$ in rather good agreement with ^{236}U and ^{232}Th . However one can not be satisfied by this agreement, because this value turns out a little bit too small in comparison with the theoretical result $5.8 \mu_N^2$. In addition, having remarkably bigger deformation, ^{238}U is expected to have bigger

TABLE VIII: The nuclear scissors mode fine structure. The results of calculations by the WFM method: energies E_i with correspondings $B_i(M1)$ -values. Energy centroids \bar{E} and summed $M1$ strength are also presented. Parameters of pair correlations: $V_0^p = 25.5$ MeV, $V_0^n = 21.5$ MeV, $r_p^n = 1.5$ fm, $r_p^n = 1.80$ fm; $\kappa_{\text{Nilis}} = 0.06$, $q = 0.7$.

Nuclei	δ	i	E_i (MeV)	$B_i(M1)$ (μ_N^2)	$\bar{E}_{[2-3]}$ (MeV)	$\sum_{i=2}^3 B_i(M1)$ [μ_N^2]		$\bar{E}_{[1-3]}$ (MeV)	$\sum_{i=1}^3 B_i(M1)$ (μ_N^2)	
			WFM	WFM	WFM	NRF	WFM	NRF	WFM	
^{232}Th	0.216	1	1.53	1.70						
		2	2.21	2.55	2.43	2.49	4.07	4.26(64)	2.16	5.77
		3	2.81	1.51						
^{236}U	0.220	1	1.54	1.91						
		2	2.22	2.87	2.44	2.35	4.51	4.06(61)	2.17	6.41
		3	2.82	1.64						
^{238}U	0.234	1	1.57	2.12						
		2	2.32	3.69	2.54	2.58	5.80	7.59(1.2)	2.28	7.92
		3	2.93	2.10						

$M1$ strength than ^{236}U and ^{232}Th according to the experimentally established rule $B(M1) \sim \delta^2$. In this connection it makes sense to consider another possible place for the required boundary. If one puts it into the less pronounced spectrum gap between 2.82 MeV and 2.88 MeV, then the summed $B(M1)$ of scissors becomes $5.97 \mu_N^2$ which agrees rather well with the theoretical value.

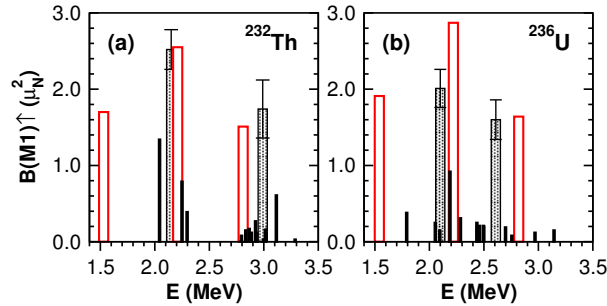


FIG. 8: The centroids of experimentally observed spectra of 1^+ excitations in ^{232}Th (a) and ^{236}U (b) (black rectangles with error bars) are compared with the results of WFM calculations (red rectangles).

C. Currents

Figure 2 gives a schematic view of all possible nuclear scissors. To obtain a more objective picture of the phenomenon it is necessary to study the distribution of neutron and proton currents $J_i^S(\mathbf{r})$. By definition the current is obtained by the odd in \mathbf{p} part of the phase space distribution

$$J_i^S(\mathbf{r}, t) = \int \frac{d^3p}{(2\pi\hbar)^3} p_i f_o^S(\mathbf{r}, \mathbf{p}, t). \quad (25)$$

An isospin index is omitted for simplicity. In Ref. [4], where the simple model of a harmonic oscillator with separable QQ interaction was considered, the analytical formula for the nucleons' flows was derived. In the case with spin degrees of freedom and pair correlations the currents can be constructed only numerically. According to the approximation suggested in [11, 25] the current variation is expanded in the following series:

$$\delta J_i^S(\mathbf{r}, t) = n^+(\mathbf{r}) \left[K_i^S(t) + \sum_j (-1)^j K_{i,-j}^S(t) r_j + \sum_{\lambda', \mu'} (-1)^{\mu'} K_{i, \lambda' - \mu'}^S(t) \{r \otimes r\}_{\lambda' \mu'} + \dots \right]. \quad (26)$$

All terms containing expansion coefficients K with odd numbers of indexes disappear due to axial symmetry. Furthermore, we truncate this series omitting all terms generating higher than second order moments. So, finally the following expression is used:

$$\delta J_i^S(\mathbf{r}, t) = n^+(\mathbf{r}) \sum_j (-1)^j K_{i,-j}^S(t) r_j. \quad (27)$$

The detailed expressions are:

$$\begin{aligned} \delta J_1^S &= n^+ (K_{1,0}^S r_0 - K_{1,-1}^S r_1 - K_{1,1}^S r_{-1}), \\ \delta J_0^S &= n^+ (K_{0,0}^S r_0 - K_{0,-1}^S r_1 - K_{0,1}^S r_{-1}), \\ \delta J_{-1}^S &= n^+ (K_{-1,0}^S r_0 - K_{-1,-1}^S r_1 - K_{-1,1}^S r_{-1}). \end{aligned}$$

The coefficients $K_{i,-j}^S(t)$ are connected by linear relations with the collective variables $\mathcal{L}_{\lambda\mu}^S(t)$ (see Appendix B). Taking into account, that in the frame of the problem considered here $\mathcal{L}_{\lambda 0}^S = \mathcal{L}_{\lambda 2}^S = 0$ for

TABLE IX: Strengths (amplitudes) of currents in ^{164}Dy . $\beta = -B/A$.

E (MeV)	(i)	B (10^{-2})	A (10^{-2})	%	β
2.20	(a)	0.75	-0.47	1.75	1.60
	(b)	0.51	-0.18		2.79
	(c)	-1.46	2.77	47.29	0.53
	(d)	2.72	-3.42		0.79
	(e)	2.87	-3.50	50.95	0.82
	(f)	-1.61	2.85		0.57
2.87	(a)	1.99	-2.44	31.90	0.82
	(b)	-2.94	4.00		0.74
	(c)	2.90	-3.32	53.71	0.87
	(d)	-3.85	4.89		0.79
	(e)	1.22	-1.24	14.39	0.99
	(f)	-2.17	2.80		0.78
3.59	(a)	11.57	-12.14	61.55	0.95
	(b)	-8.17	15.05		0.54
	(c)	-1.87	5.75	7.76	0.33
	(d)	5.27	-2.84		1.86
	(e)	-5.95	10.39	30.69	0.57
	(f)	9.35	-7.48		1.25

$\varsigma = +, -$, we find

$$\begin{aligned}\delta J_1^\varsigma &= n^+ \alpha_1 (\mathcal{L}_{21}^\varsigma - \mathcal{L}_{11}^\varsigma) r_0, \\ \delta J_0^\varsigma &= n^+ \alpha_2 [(\mathcal{L}_{2-1}^\varsigma - \mathcal{L}_{1-1}^\varsigma) r_1 + (\mathcal{L}_{21}^\varsigma + \mathcal{L}_{11}^\varsigma) r_{-1}], \\ \delta J_{-1}^\varsigma &= n^+ \alpha_1 (\mathcal{L}_{2-1}^\varsigma + \mathcal{L}_{1-1}^\varsigma) r_0,\end{aligned}$$

where $\alpha_i = \sqrt{3}/(\sqrt{2}A_i)$ and A_i are defined by (24). The expressions for currents in Cartesian coordinates are written:

$$\begin{aligned}\delta J_x^\varsigma &= (\delta J_{-1}^\varsigma - \delta J_1^\varsigma)/\sqrt{2} \\ &= \frac{1}{\sqrt{2}} n^+ \alpha_1 (\mathcal{L}_{2-1}^\varsigma - \mathcal{L}_{21}^\varsigma + \mathcal{L}_{1-1}^\varsigma + \mathcal{L}_{11}^\varsigma) z, \\ \delta J_y^\varsigma &= i(\delta J_{-1}^\varsigma + \delta J_1^\varsigma)/\sqrt{2} \\ &= \frac{i}{\sqrt{2}} n^+ \alpha_1 (\mathcal{L}_{2-1}^\varsigma + \mathcal{L}_{21}^\varsigma + \mathcal{L}_{1-1}^\varsigma - \mathcal{L}_{11}^\varsigma) z, \\ \delta J_z^\varsigma &= \delta J_0^\varsigma = n^+ \alpha_2 \left[(\mathcal{L}_{21}^\varsigma - \mathcal{L}_{2-1}^\varsigma + \mathcal{L}_{11}^\varsigma + \mathcal{L}_{1-1}^\varsigma) x \right. \\ &\quad \left. - \frac{i}{\sqrt{2}} (\mathcal{L}_{21}^\varsigma + \mathcal{L}_{2-1}^\varsigma + \mathcal{L}_{11}^\varsigma - \mathcal{L}_{1-1}^\varsigma) y \right].\end{aligned}\quad (28)$$

The comparison of the set of equations for $\mu = 1$ (22) with the analogous set of equations for $\mu = -1$ allows one to find that $\mathcal{L}_{2-1}^\varsigma = \mathcal{L}_{21}^\varsigma$ and

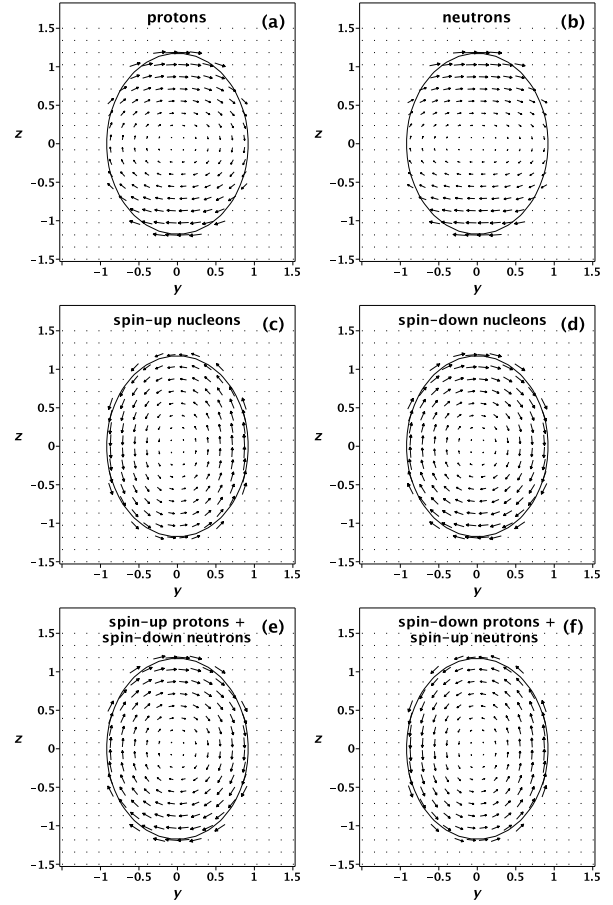


FIG. 9: The currents in ^{164}Dy for $E = 2.20$ MeV: δJ_p^+ (a), δJ_n^+ (b), $\delta J^{\uparrow\uparrow}$ (c), $\delta J^{\downarrow\downarrow}$ (d), $\delta J_p^{\uparrow\uparrow} + \delta J_n^{\downarrow\downarrow}$ (e), $\delta J_p^{\downarrow\downarrow} + \delta J_n^{\uparrow\uparrow}$ (f). $y = y/R$, $z = z/R$.

$\mathcal{L}_{1-1}^\varsigma = -\mathcal{L}_{11}^\varsigma$ (with $\varsigma = +, -$). Therefore we have:

$$\begin{aligned}\delta J_x^\varsigma &= 0, \\ \delta J_y^\varsigma &= -i \frac{\sqrt{3}}{A_1} n^+ (\mathcal{L}_{11}^\varsigma - \mathcal{L}_{21}^\varsigma) z, \\ \delta J_z^\varsigma &= -i \frac{\sqrt{3}}{A_2} n^+ (\mathcal{L}_{11}^\varsigma + \mathcal{L}_{21}^\varsigma) y.\end{aligned}\quad (29)$$

This result is quite remarkable. The first equation $\delta J_x^\varsigma = 0$ says that all motions take place only in two dimensions, i.e. in one plane. Obviously it is one of the properties to be satisfied by the scissors mode. Another obvious and necessary property of the scissors mode is the rotational out of phase motion of its subentities. This property is demonstrated by the pictures of currents (see Figs. 9, 10, 11) constructed with the help of second and third equations of (29).

Let us analyze these figures. First of all it is seen that one can not identify any of three $M1$ excitations with only one type of motions shown on Fig. 2 – it turns out that every excitation is a mixture of all three possible scissors. Nevertheless an approximate

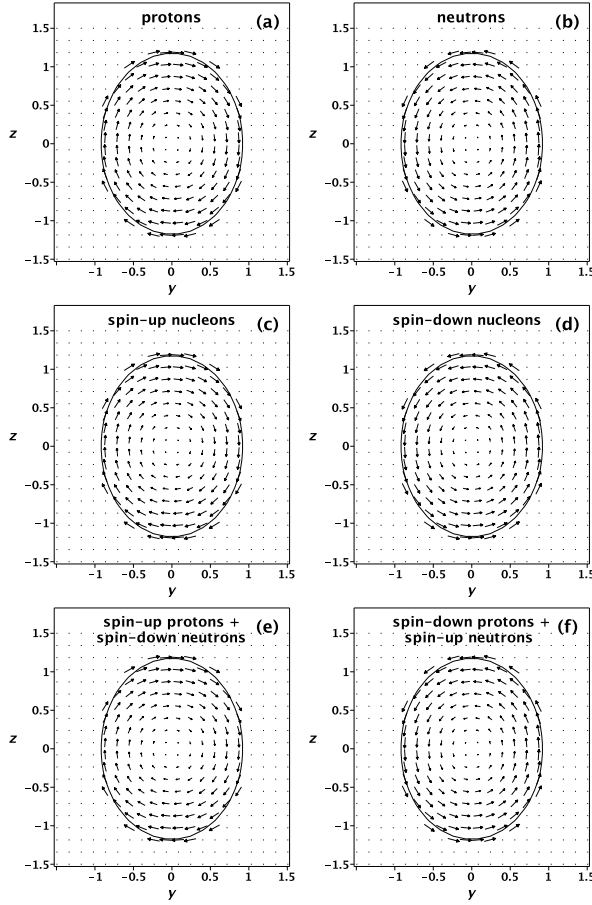


FIG. 10: The currents in ^{164}Dy for $E = 2.87$ MeV: δJ_p^+ (a), δJ_n^+ (b), $\delta J^{\uparrow\uparrow}$ (c), $\delta J^{\downarrow\downarrow}$ (d), $\delta J_p^{\uparrow\uparrow} + \delta J_n^{\downarrow\downarrow}$ (e), $\delta J_p^{\downarrow\downarrow} + \delta J_n^{\uparrow\uparrow}$ (f). $y = y/R$, $z = z/R$.

identification can be made. It is necessary to introduce some numerical measure of the contribution of every type of scissors into the particular excitation. Introducing the notations (see (29))

$$A = -i \frac{\sqrt{3}}{A_2} (\mathcal{L}_{11}^s + \mathcal{L}_{21}^s),$$

$$B = -i \frac{\sqrt{3}}{A_1} (\mathcal{L}_{11}^s - \mathcal{L}_{21}^s)$$

we can construct the following indicator characterizing the definite scissors, for example, conventional one:

$$AB_{(ab)} = [A^2 + B^2]_{(a)} + [A^2 + B^2]_{(b)}.$$

Analogous values $AB_{(cd)}$ and $AB_{(ef)}$ are defined also for spin scissors. After normalization all three values are transformed in percents, which are shown in Table IX together with the respective values of A and B . The simple analysis of this Table allows one to conclude that:

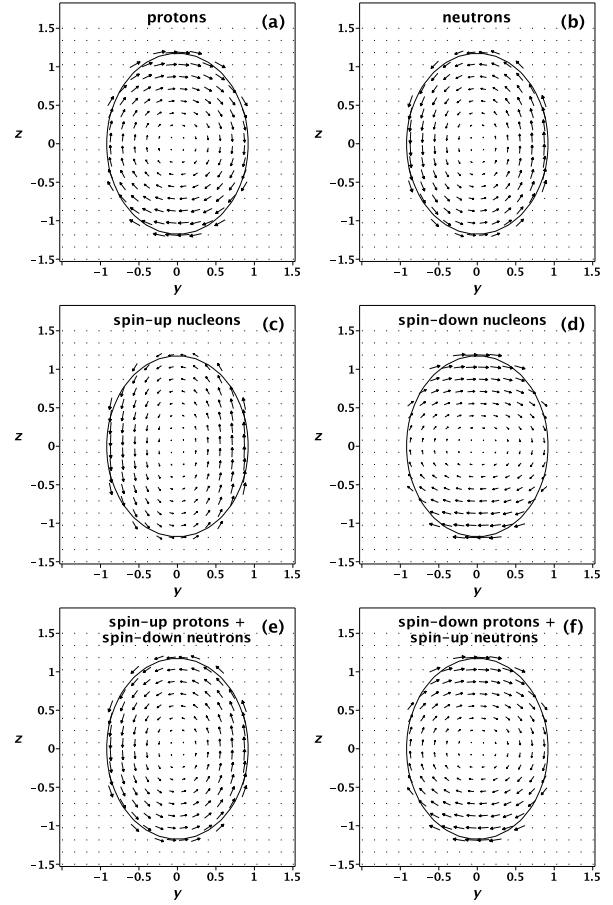


FIG. 11: The currents in ^{164}Dy for $E = 3.59$ MeV: δJ_p^+ (a), δJ_n^+ (b), $\delta J^{\uparrow\uparrow}$ (c), $\delta J^{\downarrow\downarrow}$ (d), $\delta J_p^{\uparrow\uparrow} + \delta J_n^{\downarrow\downarrow}$ (e), $\delta J_p^{\downarrow\downarrow} + \delta J_n^{\uparrow\uparrow}$ (f). $y = y/R$, $z = z/R$.

1. excitation with $E = 2.20$ MeV represents predominantly (51%) the "complicate" spin scissors (Fig. 9 (e), (f)) with rather strong admixture (47%) of the "simple" spin scissors (Fig. 9 (c), (d)),
2. excitation with $E = 2.87$ MeV represents predominantly (54%) the "simple" spin scissors (Fig. 10 (c), (d)) with rather big admixture (32%) of the conventional scissors (Fig. 10 (a), (b)),
3. excitation with $E = 3.59$ MeV represents predominantly (62%) the conventional scissors (Fig. 11 (a), (b)) with a rather strong admixture (31%) of the "complicate" spin scissors (Fig. 11 (e), (f)).

It is worth to note, that introduced in [4] indicator $\beta = -B/A$ works here too: if β is positive or negative the lines of current produce ellipse or hyperbola.

The situation with currents in Actinides is exactly the same as in Rare Earths. The picture of currents in ^{232}Th is indistinguishable from that of ^{164}Dy .

VI. CONCLUSION

We have solved the dynamical equations describing the nuclear collective motion without the artificial division into isovector and isoscalar parts, an approximation we had applied in our previous work. As a result a new, third, type of nuclear scissors is found. The three types of scissors modes can be approximately classified as isovector spin-scalar (conventional), isovector spin-vector and isoscalar spin-vector, see Fig. 2. The analysis of currents has shown that three low-lying 1^+ magnetic excitations, predicted by the theory (see Table I), represent quite strong mixture of all three scissors. The calculated energy centroids and summarized transition probabilities of even-even Dy isotopes are in very good agreement with the experimental results of the Oslo group. The experimental NRF data for ^{164}Dy are also in excellent agreement with our calculations, whereas the data for $^{160,162}\text{Dy}$ are in good agreement only with the calculated centroids of the two higher lying scissors. So we agree with the conclusion of the authors of [18]: *“It is highly desirable to remeasure the Dy isotopes by performing NRF experiments using quasi-monochromatic beams in the interesting energy region between 2 and 4 MeV as*

done for ^{232}Th .” According to our latest findings it is necessary to extend their proposal to all Rare Earth and Actinide nuclei.

More precisely, a satisfactory agreement is achieved for well deformed nuclei of the rare earth region with standard values of all possible parameters. The accuracy of the description of the scissors mode by the WFM method is comparable with that of QRPA, what is demonstrated by the comparison of our results of calculations in the frame of WFM and QPNM approaches. A satisfactory agreement is also achieved for weakly deformed (transitional) nuclei of the same region by a very modest re-fit of the spin-orbit strength. We suppose that fourth order moments and more realistic interactions are required for the adequate description of transitional nuclei. This will be the subject of future work.

Acknowledgments

Valuable discussions with M. Urban are gratefully acknowledged. The work was supported by the IN2P3/CNRS-JINR 03-57 Collaboration agreement.

Appendix A: Pairing

$$I_{pp}^{\kappa\Delta}(\mathbf{r}, p) = \frac{r_p^3}{\sqrt{\pi}\hbar^3} e^{-\alpha p^2} \int \kappa^r(\mathbf{r}, p') [\phi_0(x) - 4\alpha^2 p'^4 \phi_2(x)] e^{-\alpha p'^2} p'^2 dp', \quad (\text{A1})$$

$$I_{rp}^{\kappa\Delta}(\mathbf{r}, p) = \frac{r_p^3}{\sqrt{\pi}\hbar^3} e^{-\alpha p^2} \int \kappa^r(\mathbf{r}, p') [\phi_0(x) - 2\alpha p'^2 \phi_1(x)] e^{-\alpha p'^2} p'^2 dp', \quad (\text{A2})$$

where $x = 2\alpha p p'$,

$$\begin{aligned} \phi_0(x) &= \frac{1}{x} \sinh(x), & \phi_1(x) &= \frac{1}{x^2} \left[\cosh(x) - \frac{1}{x} \sinh(x) \right], \\ \phi_2(x) &= \frac{1}{x^3} \left[\left(1 + \frac{3}{x^2} \right) \sinh(x) - \frac{3}{x} \cosh(x) \right]. \end{aligned} \quad (\text{A3})$$

Anomalous density and semiclassical gap equation [9]:

$$\kappa(\mathbf{r}, \mathbf{p}) = \frac{1}{2} \frac{\Delta(\mathbf{r}, \mathbf{p})}{\sqrt{\hbar^2(\mathbf{r}, \mathbf{p}) + \Delta^2(\mathbf{r}, \mathbf{p})}}, \quad (\text{A4})$$

$$\Delta(\mathbf{r}, \mathbf{p}) = -\frac{1}{2} \int \frac{d^3 p'}{(2\pi\hbar)^3} v(|\mathbf{p} - \mathbf{p}'|) \frac{\Delta(\mathbf{r}, \mathbf{p}')}{\sqrt{\hbar^2(\mathbf{r}, \mathbf{p}') + \Delta^2(\mathbf{r}, \mathbf{p}')}}, \quad (\text{A5})$$

where $v(|\mathbf{p} - \mathbf{p}'|) = \beta e^{-\alpha|\mathbf{p} - \mathbf{p}'|^2}$ with $\beta = -|V_0|(r_p\sqrt{\pi})^3$ and $\alpha = r_p^2/4\hbar^2$.

The functions $\Delta(r') \equiv \Delta_{eq}(r', p_F(r'))$, $I_{rp}^{\kappa\Delta}(r') \equiv I_{rp}^{\kappa\Delta}(r', p_F(r'))$, $I_{pp}^{\kappa\Delta}(r') \equiv I_{pp}^{\kappa\Delta}(r', p_F(r'))$ depend on the radius r' and the local Fermi momentum $p_F(r')$. The value of r' is not fixed by the theory and can be used

as the fitting parameter. Nevertheless, to get rid off the fitting parameter, we use the averaged values of these functions: $\bar{\Delta} = \int d\mathbf{r} n(\mathbf{r})\Delta(r, p_F(r))/A$, etc.

Appendix B: Currents

$$\mathcal{L}_{\lambda,\mu}^s = \int d^3r \{r \otimes \delta J^s\}_{\lambda\mu} = \frac{1}{\sqrt{3}}(-1)^\lambda \left[A_1 C_{1\mu,10}^{\lambda\mu} K_{\mu,0}^s - A_2 \left(C_{1\mu+1,1-1}^{\lambda\mu} K_{\mu+1,-1}^s + C_{1\mu-1,11}^{\lambda\mu} K_{\mu-1,1}^s \right) \right]. \quad (\text{B1})$$

$$\begin{aligned} K_{-1,-1}^s &= -\frac{\sqrt{3}\mathcal{L}_{2-2}^s}{A_2}, & K_{-1,0}^s &= \frac{\sqrt{3}(\mathcal{L}_{1-1}^s + \mathcal{L}_{2-1}^s)}{\sqrt{2}A_1}, & K_{-1,1}^s &= -\frac{\sqrt{3}\mathcal{L}_{10}^s + \mathcal{L}_{20}^s + \sqrt{2}\mathcal{L}_{00}^s}{\sqrt{2}A_2}, \\ K_{0,-1}^s &= \frac{\sqrt{3}(\mathcal{L}_{1-1}^s - \mathcal{L}_{2-1}^s)}{\sqrt{2}A_2}, & K_{0,0}^s &= \frac{\sqrt{2}\mathcal{L}_{2,0}^s - \mathcal{L}_{0,0}^s}{A_1}, & K_{0,1}^s &= -\frac{\sqrt{3}(\mathcal{L}_{11}^s + \mathcal{L}_{21}^s)}{\sqrt{2}A_2}, \\ K_{1,-1}^s &= \frac{\sqrt{3}\mathcal{L}_{10}^s - \mathcal{L}_{20}^s - \sqrt{2}\mathcal{L}_{00}^s}{\sqrt{2}A_2}, & K_{1,0}^s &= \frac{\sqrt{3}(\mathcal{L}_{21}^s - \mathcal{L}_{11}^s)}{\sqrt{2}A_1}, & K_{1,1}^s &= -\frac{\sqrt{3}\mathcal{L}_{22}^s}{A_2}, \end{aligned} \quad (\text{B2})$$

where

$$A_1 = \frac{Q_{00}}{\sqrt{3}} \left(1 + \frac{4}{3}\delta \right), \quad A_2 = -\frac{Q_{00}}{\sqrt{3}} \left(1 - \frac{2}{3}\delta \right), \quad Q_{00} = A \langle r^2 \rangle = \frac{3}{5}AR^2. \quad (\text{B3})$$

Appendix C: Excitation probabilities

Excitation probabilities are calculated with the help of the theory of linear response of the system to a weak external field

$$\hat{O}(t) = \hat{O} e^{-i\Omega t} + \hat{O}^\dagger e^{i\Omega t}. \quad (\text{C1})$$

A detailed explanation can be found in [4, 6]. We recall only the main points. The matrix elements of the operator \hat{O} obey the relationship [26]

$$|\langle \psi_a | \hat{O} | \psi_0 \rangle|^2 = \hbar \lim_{\Omega \rightarrow \Omega_a} (\Omega - \Omega_a) \overline{\langle \psi' | \hat{O} | \psi' \rangle e^{-i\Omega t}}, \quad (\text{C2})$$

where ψ_0 and ψ_a are the stationary wave functions of the unperturbed ground and excited states; ψ' is the wave function of the perturbed ground state, $\Omega_a = (E_a - E_0)/\hbar$ are the normal frequencies, the bar means averaging over a time interval much larger than $1/\Omega$.

To calculate the magnetic transition probability, it is necessary to excite the system by the following external field:

$$\hat{O}_{\lambda\mu} = \mu_N \left(g_s^\tau \hat{\mathbf{S}}/\hbar - ig_l^\tau \frac{2}{\lambda+1} [\mathbf{r} \times \nabla] \right) \nabla(r^\lambda Y_{\lambda\mu}), \quad \mu_N = \frac{e\hbar}{2mc}. \quad (\text{C3})$$

Here $g_l^p = 1$, $g_s^p = 5.5856$ for protons and $g_l^n = 0$, $g_s^n = -3.8263$ for neutrons. The dipole operator ($\lambda = 1$, $\mu = 1$) in cyclic coordinates looks like

$$\hat{O}_{11} = \sqrt{\frac{3}{4\pi}} \left[g_s^\tau \hat{S}_1/\hbar - g_l^\tau \sqrt{2} \sum_{\nu,\sigma} C_{1\nu,1\sigma}^{11} r_\nu \nabla_\sigma \right] \mu_N. \quad (\text{C4})$$

Its Wigner transform is

$$(\hat{O}_{11})_W = \sqrt{\frac{3}{4\pi}} \left[g_s^\tau \hat{S}_1 - ig_l^\tau \sqrt{2} \sum_{\nu,\sigma} C_{1\nu,1\sigma}^{11} r_\nu p_\sigma \right] \frac{\mu_N}{\hbar}. \quad (\text{C5})$$

For the matrix element we have

$$\begin{aligned}
\langle \psi' | \hat{O}_{11} | \psi' \rangle &= \sqrt{\frac{3}{2\pi}} \left[-\frac{\hbar}{2} (g_s^n \mathcal{F}^{n\downarrow\uparrow} + g_s^p \mathcal{F}^{p\downarrow\uparrow}) - i g_l^p \mathcal{L}_{11}^{p+} \right] \frac{\mu_N}{\hbar} \\
&= \sqrt{\frac{3}{8\pi}} \left[-\frac{1}{2} [(g_s^n - g_s^p) \bar{\mathcal{F}}^{\downarrow\uparrow} + (g_s^n + g_s^p) \mathcal{F}^{\downarrow\uparrow}] + \frac{i}{\hbar} g_l^p (\bar{\mathcal{L}}_{11}^+ - \mathcal{L}_{11}^+) \right] \mu_N \\
&= \sqrt{\frac{3}{8\pi}} \left[\frac{1}{2} (g_s^p - g_s^n) \bar{\mathcal{F}}^{\downarrow\uparrow} + \frac{i}{\hbar} g_l^p \bar{\mathcal{L}}_{11}^+ + \frac{i}{\hbar} [g_s^n + g_s^p - g_l^p] \mathcal{L}_{11}^+ \right] \mu_N.
\end{aligned} \tag{C6}$$

Deriving (C6) we have used the relation $2i\mathcal{L}_{11}^+ = -\hbar\mathcal{F}^{\downarrow\uparrow}$, which follows from the angular momentum conservation [6].

One has to add the external field (C4) to the Hamiltonian (6). Due to the external field some dynamical equations of (22) become inhomogeneous:

$$\begin{aligned}
\dot{\mathcal{R}}_{21}^+ &= \dots + i \frac{3}{\sqrt{\pi}} \frac{\mu_N}{2\hbar} g_l^p R_{20}^{p+}(\text{eq}) e^{i\Omega t}, \\
\dot{\mathcal{L}}_{11}^- &= \dots + i \sqrt{\frac{3}{\pi}} \frac{\mu_N}{2\hbar} g_l^p L_{10}^{p-}(\text{eq}) e^{i\Omega t}, \\
\dot{\mathcal{L}}_{10}^{\downarrow\uparrow} &= \dots + i \sqrt{\frac{3}{2\pi}} \frac{\mu_N}{2\hbar} [g_s^n L_{10}^{n-}(\text{eq}) - g_s^p L_{10}^{p-}(\text{eq})] e^{i\Omega t}.
\end{aligned} \tag{C7}$$

For the isoscalar set of equations, respectively, we obtain:

$$\begin{aligned}
\dot{\mathcal{R}}_{21}^+ &= \dots - i \frac{3}{\sqrt{\pi}} \frac{\mu_N}{2\hbar} g_l^p R_{20}^{p+}(\text{eq}) e^{i\Omega t}, \\
\dot{\mathcal{L}}_{11}^- &= \dots - i \sqrt{\frac{3}{\pi}} \frac{\mu_N}{2\hbar} g_l^p L_{10}^{p-}(\text{eq}) e^{i\Omega t}, \\
\dot{\mathcal{L}}_{10}^{\downarrow\uparrow} &= \dots + i \sqrt{\frac{3}{2\pi}} \frac{\mu_N}{2\hbar} [g_s^n L_{10}^{n-}(\text{eq}) + g_s^p L_{10}^{p-}(\text{eq})] e^{i\Omega t}.
\end{aligned} \tag{C8}$$

Solving the inhomogeneous set of equations one can find the required in (C6) values of \mathcal{L}_{11}^+ , $\bar{\mathcal{L}}_{11}^+$ and $\mathcal{F}^{\downarrow\uparrow}$ and calculate $B(M1)$ factors for all excitations with the help of relationship (C2).

One also should be aware of the fact that straightforward application of Lane's formula to the present

WFM approach which leads to non-symmetric eigenvalue problems may yield negative transition probabilities violating the starting relation (C2). However, with the parameters employed here and also in our previous works [4, 6, 7, 11, 27, 28], this never happened.

-
- | | |
|--|---|
| <p>[1] K. Heyde, P. von Neumann-Cosel, and A. Richter, <i>Rev. Mod. Phys.</i> 82, 2365 (2010).</p> <p>[2] A. Richter, <i>Prog. Part. Nucl.</i> 34, 261 (1995).</p> <p>[3] U. Kneissl, H. H. Pitz, and A. Zilges, <i>Prog. Part. Nucl. Phys.</i> 37, 349 (1996).</p> <p>[4] E. B. Balbutsev and P. Schuck, <i>Nucl. Phys. A</i> 720, 293 (2003); 728, 471 (2003).</p> <p>[5] E. B. Balbutsev and P. Schuck, <i>Ann. Phys.</i> 322, 489 (2007).</p> <p>[6] E. B. Balbutsev, I.V. Molodtsova, and P. Schuck, <i>Nucl. Phys. A</i> 872, 42 (2011).</p> <p>[7] E. B. Balbutsev, I.V. Molodtsova, and P. Schuck, <i>Phys. Rev. C</i> 91, 064312 (2015).</p> <p>[8] V. G. Soloviev, <i>Theory of complex nuclei</i> (Pergamon Press, Oxford, 1976).</p> | <p>[9] P. Ring and P. Schuck, <i>The Nuclear Many-Body Problem</i> (Springer, Berlin, 1980).</p> <p>[10] D. A. Varshalovitch, A. N. Moskalev, and V. K. Khersonski, <i>Quantum Theory of Angular Momentum</i> (World Scientific, Singapore, 1988).</p> <p>[11] E. B. Balbutsev, I.V. Molodtsova, and P. Schuck, <i>Phys. Rev. C</i> 88, 014306 (2013).</p> <p>[12] M. Urban, <i>Phys. Rev. A</i> 75, 053607 (2007).</p> <p>[13] E. B. Balbutsev, I.V. Molodtsova, and P. Schuck, <i>Phys. Rev. C</i> 97, 044316 (2018).</p> <p>[14] N. Pietralla, P. von Brentano, R.-D. Herzberg, U. Kneissl, J. Margraf, H. Maser, H. H. Pitz, and A. Zilges, <i>Phys. Rev. C</i> 52, R2317 (1995).</p> <p>[15] J. Enders, P. von Neumann-Cosel, C. Rangacharyulu, and A. Richter, <i>Phys. Rev. C</i> 71,</p> |
|--|---|

- 014306 (2005).
- [16] N. Pietralla, P. von Brentano, R.-D. Herzberg, U. Kneissl, N. Lo Iudice, H. Maser, H. H. Pitz, and A. Zilges, *Phys. Rev. C* **58**, 184 (1998).
 - [17] J. Margraf, T. Eckert, M. Rittner, I. Bauske, O. Beck, U. Kneissl, H. Maser, H. H. Pitz, A. Schiller, P. von Brentano, R. Fischer, R.-D. Herzberg, N. Pietralla, A. Zilges, and H. Friedrichs, *Phys. Rev. C* **52**, 2429 (1995).
 - [18] T. Renstrøm, H. Utsunomiya, H. T. Nyhus, A. C. Larsen, M. Guttormsen, G. M. Tveten, D. M. Filipescu, I. Gheorghe, S. Goriely, S. Hilaire, Y.-W. Lui, J. E. Midtbø, S. Péru, T. Shima, S. Siem, and O. Tesileanu, *Phys. Rev. C* **98**, 054310 (2018).
 - [19] V. G. Soloviev, A. V. Sushkov, N. Yu. Shirikova, and N. Lo Iudice, *Nucl. Phys. A* **600**, 155 (1996).
 - [20] V. G. Soloviev, A. V. Sushkov, and N. Yu. Shirikova, *Phys. Part. Nucl.* **31**(4), 385 (2000).
 - [21] S. Valenta, B. Baramsai, T. A. Bredeweg, A. Couture, A. Chyzh, M. Jandel, J. Kroll, M. Krτίčka, G. E. Mitchell, J. M. O'Donnell, G. Rusev, J. L. Ullmann, and C. L. Walker, *Phys. Rev. C* **96**, 054315 (2017).
 - [22] A. S. Adekola, C. T. Angell, S. L. Hammond, A. Hill, C. R. Howell, H. J. Karwowski, J. H. Kelley, and E. Kwan, *Phys. Rev. C* **83**, 034615 (2011).
 - [23] J. Margraf, A. Degener, H. Friedrichs, R. D. Heil, A. Jung, U. Kneissl, S. Lindenstruth, H. H. Pitz, H. Schacht, U. Seemann, R. Stock, C. Wesselborg, P. von Brentano, and A. Zilges, *Phys. Rev. C* **42**, 771 (1990).
 - [24] S. L. Hammond, A. S. Adekola, C. T. Angell, H. J. Karwowski, E. Kwan, G. Rusev, A.P. Tonchev, W. Tornow, C. R. Howell, and J. H. Kelley, *Phys. Rev. C* **85**, 044302 (2012).
 - [25] E. B. Balbutsev, *Sov. J. Part. Nucl.* **22**, 159 (1991).
 - [26] A. M. Lane, *Nuclear Theory* (Benjamin, New York, 1964).
 - [27] E. B. Balbutsev, L. A. Malov, P. Schuck, M. Urban, and X. Viñas, *Phys. At. Nucl.* **71**, 1012 (2008).
 - [28] E. B. Balbutsev, L. A. Malov, P. Schuck, and M. Urban, *Phys. At. Nucl.* **72**, 1305 (2009).